ISSN 0915-633X

NATIONAL INSTITUTE FOR FUSION SCIENCE

Interplay of Energetic Ions and Alfvén Modes in Helical Plasmas

Ya. I. Kolesnichenko, K. Yamazaki, S. Yamamoto, V.V. Lutsenko, N. Nakajima,
Y. Narushima, K. Toi, Yu. V. Yakovenko

(Received - July 7, 2003)

NIFS-781 Aug. 2003

This report was prepared as a preprint of work performed as a collaboration research of the National Institute for Fusion Science (NIFS) of Japan. The views presented here are solely those of the authors. This document is intended for information only and may be published in a journal after some rearrangement of its contents in the future.

Inquiries about copyright should be addressed to the Research Information Center, National Insitute for Fusion Science, Oroshi-cho, Toki-shi, Gifu-ken 509-5292 Japan.

E-mail: bunken@nifs.ac.jp

<Notice about photocopying>

In order to photocopy any work from this publication, you or your organization must obtain permission from the following organizaion which has been delegated for copyright for clearance by the copyright owner of this publication.

Except in the USA

Japan Academic Association for Copyright Clearance (JAACC)
41-6 Akasaka 9-chome, Minato-ku, Tokyo 107-0052 Japan
TEL:81-3-3475-5618 FAX:81-3-3475-5619 E-mail:naka-atsu@muj.biglobe.ne.jp

In the USA

Copyright Clearance Center, Inc.
222 Rosewood Drive, Danvers, MA 01923 USA
Phone: (978) 750-8400 FAX: (978) 750-4744

TOKI, JAPAN

Interplay of energetic ions and Alfvén modes in helical plasmas

Ya. I. Kolesnichenko*, K. Yamazaki**, S. Yamamoto***, V. V. Lutsenko*,

N. Nakajima**, Y. Narushima**, K. Toi**, Yu. V. Yakovenko*

*Institute for Nuclear Research, Prospekt Nauky 47, 03680 Kyiv, Ukraine

**National Institute for Fusion Science, Oroshi-cho 322-6, Toki, 509-5292, Japan

***Department of Energy Engineering and Science,

Nagoya University, Nagoya-shi 464-8603, Japan

(June 24, 2003)

Abstract

Alfvén eidenmodes and their destabilization by energetic ions in stellarators, mainly, in the Large Helical Device (LHD) plasmas, are considered. A general expression for the instability growth rate is derived, which generalizes that obtained in Ref. [*Ya.I. Kolesnichenko et al., Phys. Plasmas* **9**, *517 (2002)*] by taking into account the finite magnitude of the perturbed longitudinal magnetic field. The structures of the Alfvén continuum and Alfvén eigenmodes, as well as the resonances of the wave-particle interaction, are studied. A numerical simulation of the destabilization of Alfvén waves with low mode numbers during neutral-beam injection in a particular LHD shot is carried out. The obtained solutions represent even and odd core-localized Toroidicity-induced Alfvén Eigenmodes, the calculated frequencies and the mode numbers being in agreement with experimental data. The growth rates of the instabilities are calculated.

This work was done during the stay of Ya.I. Kolesnichenko in NIFS as a Guest Professor from January 26, 2003 to April 25, 2003.

Key words:

helical plasma, Alfvén eigenmodes, Alfvén continuum, energetic ions, growth rate

I. INTRODUCTION

Alfvén instabilities (AI) caused by energetic ions were observed in many experiments on tokamaks.[1] Various Alfvén modes were destabilized also in stellarators.[2,3] These instabilities arise because of the resonant interaction between energetic ions and Alfvénic perturbations. Depending on plasma characteristics, the same resonances can lead to the destabilization of either Alfvén Eigenmodes (AE) or Energetic Particle Modes (EPM). The frequencies of AEs lie in the gaps of the Alfvén Continuum (AC), whereas frequencies of EPM lie in AC but close to the gaps. Therefore, to know AC is important for explaining experimental data and making predictive calculations.

A joint feature of AC in all stellarators is the presence of gaps caused by the break of the axial symmetry of the magnetic configuration. This leads to appearance of AEs which are absent in tokamaks.[4–7] Note that such gaps are present in AC of the so-called "quasi-axisymmetric" stellarators as well because in these systems only the magnetic field strength is symmetric in flux coordinates, but not the plasma configuration. On the other hand, different stellarators have different plasma shaping and different characteristics of the magnetic field (shear, rotational transform, Fourier harmonics of the magnetic field strength). Furthermore, different shots in the same machine, especially, in Large Helical Device[8] (LHD), may have very different characteristics of the magnetic configuration, which leads to different ACs.

Due to the mentioned gaps, high-frequency AIs associated with the destabilization of various Helicity-induced Alfvén Eigenmodes (HAE instabilities) and Mirror-induced Alfvén eigenmodes (MAE instability) can arise in stellarator plasmas in addition to the Toroidicity-induced Alfvén Eigenmode (TAE) instability. This was shown in Refs.[9,10], where AIs in a Helias reactor[11] were considered. High-frequency AIs were observed in experiments on LHD and Wendelstein 7-AS (W7-AS[12]), but only recently they were identified as HAE and MAE instabilities.[14–16] Moreover, detailed analyses of the instabilities in the cited works are absent, so that further work is required for reliable conclusions. Note that AIs in stellarators may differ from those in tokamaks not only because different Alfvén modes can be excited. Another important circumstance is that the res-

onant wave-particle interaction in stellarators has peculiarities caused by the fact that the toroidicity is not the only factor that determines the particle drift motion. Because of this, there exist "non-axisymmetric" resonances in stellarators, which dominate under certain conditions.[9,10]

In this work, we further develop the general theory of AIs in stellarators and study AIs in a particular shot of LHD, namely, the shot #24512. In the mentioned shot, low-mode-number AIs were observed, as was reported in Refs.[15,17]. The work contains various components of the analysis required for the identification of the AIs: the structure of Alfvén continuum is calculated, and the main gaps are identified; the spatial structure of AEs is considered; the resonances of the wave-particle interaction are analyzed; the growth rates of AIs are calculated.

The structure of the work is as follows. In Sec. II we present a qualitative picture of the AC and AE structure and analyze the existence of the multi-harmonic structure of AEs; in addition, we determine the relevant resonant velocities of circulating energetic ions in stellarators. In Sec. III an expression for the instability growth rate driven by the circulating energetic ions is derived. It generalizes a corresponding expression of Ref.[9] by taking into account the finite magnitude of the perturbed longitudinal magnetic field. Section IV deals with AIs observed in the LHD shot #24512. In this section the experimental results are briefly described, and numerical calculations of the mode structure and the instability growth rate are carried out. Finally, Sec. V summarizes the obtained results and contains the conclusions drawn.

II. ALFVÉN MODES AND THEIR DESTABILIZATION: QUALITATIVE ANALYSIS

A. Alfvén continuum, gap modes and their structure

If the plasma were a cylinder, the dependence of $\omega_A \equiv |k_\parallel| v_A$ ($k_\parallel$ is the longitudinal wave number, v_A is the Alfvén velocity) on the radial coordinate, r, would determine an Alfvén continuum in the frequency bar $\Delta\omega$ given by $\omega_{A,min} \leq \Delta\omega \leq \omega_{A,max}$. Spatial

inhomogeneity of the magnetic field strength and plasma shaping affect AC. First of all, AC is affected in the points r_* where the pairs of cylindrical branches of AC, $\omega_{A1}(r)$ and $\omega_{A2}(r)$ intersect. Near these points a reconnection of the branches takes place, which produces the gaps in AC where AEs can reside. Due to this, a simple and vivid picture of possible frequencies of Alfvén gap modes, i.e., the modes that can be destabilized by the energetic ions most easily, can be obtained by considering the intersection points of the cylindrical branches of AC.

Let us obtain such a picture for LHD. This stellarator is characterized by a rather large number of the field periods along the large azimuth of the torus, $N = 10$, and the considerable magnetic shear: the rotational transform $\iota(r)$ typically varies from $\iota \sim 0.4$ at the magnetic axis to $\iota \gtrsim 1$ at the edge.

We proceed from the general Fourier expansions of the perturbation, $\widetilde{X}$, the magnetic field, B, and a contravariant component of the metric tensor given by

$$\widetilde{X} = \sum_{m,n=-\infty}^{\infty} X_{m,n}(r) \exp(im\vartheta - in\varphi - i\omega t), \tag{1}$$

$$B = \bar{B}\left[1 + \frac{1}{2}\sum_{\mu,\nu=-\infty}^{\infty} \epsilon_B^{(\mu\nu)}(r) \exp(i\mu\vartheta - i\nu N\varphi)\right], \tag{2}$$

$$g^{\psi\psi} = \bar{g}\left[1 + \frac{1}{2}\sum_{\mu,\nu=-\infty}^{\infty} \epsilon_g^{(\mu\nu)}(r) \exp(i\mu\vartheta - i\nu N\varphi)\right], \tag{3}$$

where $g^{\psi\psi} = |\nabla\psi|^2$; $(\psi,\ \vartheta,\ \varphi)$ are Boozer flux coordinates with ψ the toroidal magnetic flux; ϑ and φ are the poloidal and toroidal coordinates, respectively; $\bar{B}$ is the average magnetic field at the magnetic axis; the radial coordinate r is defined by $\psi = \bar{B}r^2/2$; m and n are the poloidal and toroidal mode numbers, respectively, $\epsilon_{B,g}^{(-\mu,-\nu)} = \epsilon_{B,g}^{(\mu,\nu)*}$. Let us consider a pair of Fourier harmonics of the perturbation with the mode numbers m, n and $m+\mu,\ n+\nu N$. Taking $\omega_A(\iota^*, m, n,) = \omega_A(\iota^*, m+\mu, n+\nu N)$ and using $k_\parallel = (m\iota - n)/R_0$ with R_0 the radius of the magnetic axis, we easily obtain ι_* (or r_*) and the characteristic frequencies $\omega_* = |k_\parallel(r_*)|v_A(r_*)$ as follows:[6]

$$\omega_* = |k_*^{\mu\nu}|\, v_{A*}, \tag{4}$$

$$\iota_* = \frac{2n + \nu N}{2m + \mu}, \tag{5}$$

where "$*$" denotes magnitudes at $r = r_*$, $k^{\mu\nu} = (\mu\iota - \nu N)/(2R_0)$; below we will also use the normalized quantity $\tilde{k}^{\mu\nu} = k^{\mu\nu} R_0$.

The characteristic frequencies ω_* in an LHD plasma with the dominant coupling numbers $(\mu, \nu) = (1,0), (2,0), (2,1), (3,1), (1,1)$ are shown in Fig. 1. We observe that the frequency regions associated with the axisymmetric Fourier harmonics of B and $g^{\psi\psi}$ ($\nu = 0$) and the non-axisymmetric harmonics ($\nu \neq 0$) are well separated, more than in other machines, cf. Ref.[6]. This is a consequence of the fact that LHD is characterized by rather large N (for comparison: $N = 5$ in W7-AS and Wendelstein 7-X[12]). However, we should note that Fig. 1 does not show the gap width, which can be considerable. In addition, it does not take into account that in reality the gaps can be shifted up or down because of the mutual influence and the large magnitudes of coupling parameters. The mentioned effect can be significant in the periphery region of LHD plasmas, see Sec. IV.

A frequency gap around ω_* is located at r_*, and in this sense this is a "local" gap. It is of importance that ω_* does not depend explicitly on the mode numbers m, n but depends on them through r_* determined by Eq. (5). Because of this, for given (μ, ν), no continuum branches can approach ω_*, which implies that there is an empty space around $\omega_*(r_*)$, i.e., a "global" gap formed as an envelop of the infinite number of the local gaps located at various r_*.

Formally, a gap mode consists of the infinite number of Fourier harmonics. However, in practice, there are only several considerable harmonics. Furthermore, in some cases, (for instance, in Wendelstein 7-X and a Helias reactor) only a pair of coupled harmonics dominate.[6,10]

It is of interest to know the conditions of when the structure of a gap mode is multi-harmonic. Below we obtain them, assuming that there is only one dominant pair of coupling numbers (μ, ν). Then the radial profile of a corresponding eigenmode will have maxima at the points satisfying Eq. (5). Let us calculate the distance between the maxima. With this purpose we consider a pair of harmonics with the mode numbers m_0, n_0 and m_1, n_1, such that their normalized longitudinal wave numbers are $\tilde{k}_0 = m_0\iota - n_0$ and

$\widetilde{k}_1 = m_1\iota - n_1 = \widetilde{k}_0 + \Delta$ with $\Delta = \mu\iota - \nu N$. The condition $\widetilde{k}_0 + \widetilde{k}_1 = 0$ defines ι_0 given by Eq. (5) with $m = m_0$, $n = n_0$. In this point $\widetilde{k}_0 = -\Delta/2$ and $\widetilde{k}_1 = \Delta/2 = \widetilde{k}^{\mu\nu}$. Similarly, we can consider the pair m_1, n_1 and m_2, n_2, etc. In general, for the pair m_s, n_s and m_{s+1}, n_{s+1} (s an integer) we obtain $k_s = -k^{\mu\nu}(\iota_s)$, where $\iota_s = (n_s + \nu N/2)/(m_s + \mu/2)$. This leads to

$$\iota_s = \frac{n_0 + (s+0.5)\nu N}{m_0 + (s+0.5)\mu}, \tag{6}$$

and

$$\iota_{s+1} - \iota_s = \frac{\nu N m_s - \mu n_s}{(m_s + \mu/2)(m_s + 3\mu/2)}. \tag{7}$$

Equation (7) can be written as follows:

$$\frac{\iota_{s+1} - \iota_s}{\iota_s} = \frac{(\nu N m_s - \mu n_s)\iota_{s+1}}{(n_s + \nu N/2)(n_s + 3\nu N/2)}. \tag{8}$$

In order to analyze Eq. (8), we consider separately two cases, $\nu = 0$ and $\nu \neq 0$.

At first, we take $\nu = 0$. Then

$$\frac{\iota_{s+1} - \iota_s}{\iota_s} = -\iota_{s+1}\frac{\mu}{n_s}. \tag{9}$$

In weak-shear systems (Wendelstein 7-X, a Helias reactor) with $\iota \sim 1$, $[\iota(a) - \iota(0)]/\iota(0) \ll 1$, where a is the plasma radius, the left-hand side of Eq. (9) is much less than unity, whereas the right-hand side is not small for $n \sim 1$, $\iota \sim 1$. Therefore, in such systems a gap mode with $n \sim 1$, $\nu = 0$ consists of a single pair of wave harmonics. Let us assume that $|r_{s+1} - r_s| \ll r_s$. Then, writing $\iota_{s+1} - \iota_s = -\hat{s}\iota_s(r_{s+1} - r_s)/r_s$ and using Eq. (9), we obtain:

$$\frac{r_{s+1} - r_s}{r_s} = \frac{\mu}{n_s}\frac{\iota_{s+1}}{\hat{s}} \ll 1. \tag{10}$$

As expected, Eq. (10) requires a significant shear, especially, for $n \sim 1$ modes. It can be most easily satisfied for low ι (high safety factor), which is typical for tokamaks and many stellarators (in particular, for core plasmas in LHD). However, Eq. (10) represents a necessary but not sufficient condition for the multi-component structure of the mode. Another important condition is that, at least, several local frequency gaps for different s

must overlap, which implies that ω_* must be approximately constant in the region where the mode is localized. This is often the case in tokamaks but not in stellarators, where ι typically increases with the radius [the made statement becomes clear if we take into account that $\omega_* \propto \iota(r_*)/\sqrt{n_i(r_*)}$ with n_i the ion density]. We conclude from here that a multi-component $\nu = 0$ AE (for instance, a TAE mode, which sometimes is called a "global" TAE because it occupies a significant region in a plasma) typically cannot exist in stellarators. As an example, we consider the $n = 2$ TAE gap in LHD shot #24512, see Fig. 2. We observe that the local gap frequencies considerably grow with the radius even in the region where the plasma density is almost homogeneous. As a result, the "global" gap is closed, i.e., any straight line inside a local gap strikes AC in the vicinity of the local maximum located to the right.

Now we proceed to the case of $\nu \neq 0$. It follows from Eqs. (7) and (8) that the condition $|r_{s+1} - r_s| \ll r_s$ is satisfied for

$$\hat{s} \gg \left| \frac{\nu N m_s - \mu n_s}{(m_s + 1.5\mu)(n_s + 0.5\nu N)} \right|. \tag{11}$$

Equation (11) requires unrealistically large shear unless $n \gg \nu N$. On the other hand, the condition $\omega_* \approx$ const is well satisfied in a wide region for MAEs and HAEs unless the plasma density strongly changes in this region. Therefore, multi-component "global" MAEs and HAEs are possible when the mode numbers are very high. When $n < N$, a mode with $\nu \neq 0$ consists of only one pair of dominant harmonics.

The presence of several considerable coupling parameters ($\epsilon^{(\mu_l \nu_l)}$ with l the integer), as we have already mentioned, shifts the gaps in AC and, thus, affects the eigenfrequencies. In addition, it complicates the harmonic structure of AEs in stellarators, leading to "compound modes".[13] However, the dominant Fourier harmonics are those associated with the particular coupling parameter responsible for the gap. This was shown in Ref.[13] by considering the influence of the largest coupling parameter [the helical parameter $\epsilon^{(21)}$] on MAE modes in a Helias reactor. Therefore, one can say that the compound modes consist of main harmonics and satellite harmonics.

B. Resonant circulating particles

The particle magnetic drift motion in stellarators, in contrast to tokamaks, is determined by many Fourier harmonics of the magnetic field strength. Therefore, in general, there are many groups of the resonant energetic ions that drive Alfvén instabilities in stellarators. In current experiments on stellarators with the neutral beam injection, the population of the energetic ions consists mainly of circulating particles. Therefore, below we restrict ourselves to these particles. Then the resonance condition can be written as follows:[9,10]

$$\omega = [(m_s \pm \mu_r)\iota(r) - (n_s \pm \nu_r N)]v_{\|}^{res}, \tag{12}$$

where ω is the mode frequency; m_s and n_s are the mode numbers defined in Sec. II A; $v_{\|}^{res}$ is the longitudinal resonant velocity; μ_r and ν_r, $r = 1, 2, 3, \ldots$, are the "resonance" coupling numbers, i.e., the numbers characterizing Fourier harmonics of the magnetic field. Each equation corresponding to a given subscript "r" represents a resonance associated with one of the harmonics of B.

The magnitude of ω for a gap mode depends on the location of a corresponding gap in the Alfvén continuum. Let us assume that the mode consists of several considerable Fourier harmonics coupled by the only set of the coupling numbers, (μ, ν). Then the mode amplitude will have maxima located at r_s determined by Eq. (5). In these maxima Eq. (12) can be written as

$$\omega = [-k^{\mu\nu}(r_s) \pm 2k_r(r_s)]v_{\|}^{res}, \tag{13}$$

where $k_r = (\mu_r\iota - \nu_r N)/(2R_0)$, $k^{\mu\nu} = (\mu\iota - \nu N)/(2R_0)$. Note that when obtaining Eq. (13), we have taken into account that $m_s\iota_s - \nu_s N = -(\mu\iota_s - \nu N)/2$. We assume that the gap is narrow. Then there is a point r_0 where one of the maxima of the mode amplitude is located and where $\omega \approx |k^{\mu\nu}(r_0)|v_A(r_0)$. Combining this equation with Eq. (13), we obtain the resonant velocity as

$$v_{\|}^{res} = -v_A(r_0)\left[1 \pm 2\frac{k_r(r_s)}{k^{\mu\nu}(r_s)}\right]^{-1}\frac{|k^{\mu\nu}(r_0)|}{k^{\mu\nu}(r_s)}. \tag{14}$$

Note that in the particular case of a well-localized TAE mode in an axisymmetric plasma, Eq. (14) yields a well-known result, $|v_\parallel^{res}| = v_A$ and $|v_\parallel^{res}| = v_A/3$. It follows from Eq. (14) that TAEs with a multi-harmonic structure can considerably interact also with particles having the resonant velocities larger/smaller than v_A and $v_A/3$ by a factor of ι_0/ι_s [when $k_r(r_s) = k^{\mu\nu}(r_s)$].

Equation (14) describes the influence of the finite width of the region where a mode is localized, Δr_{mode}, on the resonant velocities. Below we show that finite Δr_{mode} can be important even when the mode consists of a single pair of Fourier harmonics. With this purpose, let us consider a well-localized TAE mode and assume that the maximum velocity of the energetic ions, v_0, is less than Alfvén velocity. Taking $\omega = |m\iota_* - n|v_{A*}/R_0$, we obtain from Eq. (12):

$$v_\parallel^{res} = -\frac{v_{A*}}{[1 + 2\delta(r)]} \frac{|m\iota_* - n|}{[m\iota(r) - n]}, \tag{15}$$

where $\delta(r) = \mp 0.5\iota/(m\iota - n) - 1$. One can see that there exist the mode numbers m, n for which $\delta(r_*) = 0$ and $|v_\parallel^{res}(r_*)| = v_{A*} > v_0$. This implies that there are no resonant particles at $r = r_*$ for these mode numbers. However, $\delta(r_*) \neq 0$ when $r \neq r_*$, which can provide the fulfillment of the resonance condition in the case of $\delta(r) > 0$ in the region inside Δr_{mode}. For instance, $\iota_* = 0.4$ for the TAE mode with $m = -3, -2$ and $n = -1$. The counter-propagating beam particles ($v_\parallel < 0$) can interact with the $m = -2$ harmonic at $r = r_*$ only through the resonance $v_\parallel^{res} = -v_A$. Therefore, when $v_0 < v_A$, no interaction at $r = r_*$ occurs, whereas an interaction is possible in the region where $0.4 < \iota < 0.5$. Such an interaction plays an important role in an LHD shot considered in Sec. IV.

It is of interest to determine the velocities resonant to various gap modes (in particular, TAE, EAE, and HAE_{21} modes) in LHD. We consider the case when the dominant Fourier harmonics of B are the toroidal harmonic [$\epsilon_B^{(10)}$] and three helical harmonics [$\epsilon_B^{(21)}$, $\epsilon_B^{(31)}$, $\epsilon_B^{(11)}$]. We restrict ourselves to the consideration of the "local" resonance [assuming that $|k^{\mu\nu}(r_0)| = |k^{\mu\nu}(r_s)|$]. The obtained dependencies of the resonance velocities on the pitch-angle parameter $\lambda = \mu_p \bar{B}/\mathcal{E}$ (μ_p is the particle magnetic moment, $\mathcal{E}$ is the particle energy) are shown in Fig. 3. We conclude from this figure that the torodicity-induced resonance determines the destabilization of the low-frequency instabilities (TAE, EAE) because the

resonant velocities associated with helicity are very low (which is explained by large N in LHD). However, "non-axisymmetric resonances" associated with $\epsilon_B^{(21)}$ dominate the interaction of the energetic ions and the high-frequency AEs provided that $\epsilon_B^{(21)}$ is the largest Fourier harmonic of the magnetic field.

III. GENERAL EXPRESSION FOR THE GROWTH RATE OF ALFVÉN INSTABILITIES

The instability growth rate, γ, is determined by the competition between the drive produced by energetic ions and various damping mechanisms. In the linear perturbative theory the drive and the damping are represented by additive terms in γ. Due to this fact, it is possible to treat the drive and the damping independently. Below we calculate the driving part of the growth rate, γ_α.

It is known that the ideal-MHD AEs are marginally stable, which implies that $\int d^3x\, \widetilde{\mathbf{E}} \cdot \widetilde{\mathbf{j}}^{MHD} = 0$, where $\widetilde{\mathbf{j}}^{MHD}$ is the bulk plasma current induced by the waves, the tilde labels the perturbed quantities, and the integral is taken over the plasma volume. On the other hand, the electric field of the Alfvén waves of interest (characterized by $k_\parallel \ll k_\perp$) is approximately potential, $\widetilde{\mathbf{E}} \approx -\nabla\widetilde{\Phi}$ with Φ the scalar potential. For such waves, as follows from the equation $\nabla\times\widetilde{\mathbf{B}} = 4\pi c^{-1}\widetilde{\mathbf{j}}$ ($\mathbf{j}$ is the total electric current density), the scalar product of $\widetilde{\mathbf{B}}$ and $\widetilde{\mathbf{j}}$ also vanishes provided that the radiation from the plasma is negligible:

$$\int d^3x\, \widetilde{\mathbf{E}} \cdot \widetilde{\mathbf{j}} = 0. \tag{16}$$

Therefore, when the influence of energetic ions on AEs is small, the instability growth rate can be calculated perturbatively by using Eq. (16). Writing $\omega = \omega_0 + \delta\omega$ (ω_0 is the eigenfrequency in the absence of the energetic ions, $\delta\omega \ll \omega_0$) and taking $\mathbf{j} = \mathbf{j}^{MHD} + \mathbf{j}^\alpha$ (the superscript "α" labels the energetic ion quantities) we obtain from Eq. (16), cf. Ref.[9]:

$$\delta\omega = -\frac{\int d^3x\, \widetilde{\mathbf{j}}^\alpha \cdot \mathbf{E}}{\int d^3x\, (\partial\widetilde{\mathbf{j}}^{MHD}/\partial\omega_0)\cdot\widetilde{\mathbf{E}}} = -\frac{2\pi i}{c^2}\frac{\int d^3x\, \widetilde{\mathbf{j}}^\alpha \cdot \mathbf{E}}{\sum_{m,n}\int d^3x\, \bar{v}_A^{-2}\left[|\Phi'_{m,n}|^2 + (m^2/r^2)|\Phi_{m,n}|^2\right]}, \tag{17}$$

where $\Phi'_{m,n} \equiv \partial\Phi_{m,n}/\partial r$ with r defined in Sec. II A, $\bar{v}_A = \bar{B}/\sqrt{4\pi n_i M_i}$ with n_i and M_i are the ion density and mass, respectively. Note that when obtaining the denominator

in Eq. (17), we used Eq. (1) and an equation for the ideal-MHD Alfvén eigenmodes in stellarators.[6,9]

Alfvén instabilities are usually driven by the spatial inhomogeneity of energetic ions, but the velocity anisotropy can play an important role, too. Thus, we need to know both spatial and velocity distributions of the energetic ions. The equilibrium distribution function of the energetic ions, f_0, depends on the constants of motion: $F_0 = F_0(\mathcal{E}, \mu_p, J, \sigma)$, where $\sigma = v_\parallel/|v_\parallel|$, μ_p is the particle magnetic moment (drift invariant), and J is the invariant depending on the magnetic configuration. We have to specify J. When the number of the field periods, N, is large, the drift invariant of the motion of circulating particles can be obtained by averaging the drift toroidal angular momentum over the field modulation, which yields[19] $J^{gc} = \psi_p^{gc} - 4\pi^{-1}\sigma B_3\sqrt{r\mu_p\bar{B}/(R_0 M)}\kappa_p E(\kappa_p^{-1})/\bar{\omega}_B$, where the superscript "gc" means that a quantity is taken at the particle guiding center, ψ_p is the poloidal magnetic flux, B_3 is a covariant component of $\mathbf{B}$, $\omega_B = eB/(Mc)$, $\bar{\omega}_B = \omega_B(\bar{B})$, κ_p is the particle trapping parameter. For the well circulating particles $\kappa_p^2 \approx MR_0 v_\parallel^2/(4r\mu_p B_0)$, which leads to $J^{gc} \approx \psi_p^{gc} - B_3 v_\parallel/\bar{\omega}_B$. Now we note that $\psi_p^{gc} = \psi_p + \iota(\mathbf{v}\times\mathbf{b})^1/\omega_B$ with $\mathbf{b} = \mathbf{B}_0/B_0$, the superscript "1" denoting a contravariant component of the vector. Then we obtain $J \approx \psi_p - v_3 B/\omega_B$. Thus, the motion of the well circulating particles in stellarators with the large number of the field periods can be described by the toroidal angular momentum, as in the case of axisymmetric magnetic configurations.

In Eq. (17) $\tilde{\mathbf{j}}^\alpha = \int d^3v\, \mathbf{v}\tilde{F}$, where F is the distribution function of the energetic ions. In order to find $\tilde{F}$, we proceed from the following linearized collisionless kinetic equation:

$$\frac{\partial\tilde{F}}{\partial t} + \mathbf{v}\cdot\frac{\partial\tilde{F}}{\partial\mathbf{r}} + \frac{e}{Mc}(\mathbf{v}\times\mathbf{B_0})\cdot\frac{\partial\tilde{F}}{\partial\mathbf{v}} = -\frac{e}{M}\left(\tilde{E}^i + \frac{1}{c}(\mathbf{v}\times\tilde{\mathbf{B}})^i\right)\left(Mv_i\frac{\partial F_0}{\partial\mathcal{E}} + \frac{\partial\mu_p}{\partial v^i}\frac{\partial F_0}{\partial\mu_p} - \frac{B_0}{\bar{\omega}_B}g_{3i}\frac{\partial F_0}{\partial J}\right), \tag{18}$$

where the subscript "0" labels the quantities in the unperturbed state. It is convenient to use Lagrangean coordinates, in which case $d\mathbf{r}/dt = \mathbf{v}$ and $d\mathbf{v}/dt = \mathbf{v}\times\mathbf{B}_0 e/(Mc)$. Then we can write:

$$\mathbf{v} = \mathbf{v}_\parallel + \mathbf{v}_D + \mathbf{v}_L, \tag{19}$$

$$\widetilde{\mathbf{X}}(\mathbf{r}) = \widetilde{\mathbf{X}}(\mathbf{r}_{gc}) + \frac{\partial\widetilde{\mathbf{X}}}{\partial r_{gc}^j}r_L^j, \tag{20}$$

where $\mathbf{v}_D$ is the particle drift velocity, $\mathbf{v}_L = v_L(\mathbf{e}_n \cos\alpha + \mathbf{e}_b \sin\alpha)$ is the velocity of the Larmor rotation, α is the phase of the rotation, $\mathbf{e}_n$ and $\mathbf{e}_b$ are the unit vectors along the normal and binormal to the field line, respectively, $\mathbf{r}_L = \omega_B^{-1}\mathbf{b}\times\mathbf{v}_L$ is the vector Larmor radius. Using Eqs. (19), (20) and the fact that $\tilde{E}_\parallel = 0$ for the ideal MHD waves, we write Eq. (18) in the form:

$$M\frac{d}{dt}\left(\tilde{F} + \mu_p\frac{\partial F_0}{\partial \mu_p}\frac{\widetilde{B_\parallel}}{B} + \frac{c}{i\omega}\frac{\partial F_0}{\partial J}\tilde{E}_3\right) = -\left(e\mathbf{v}_D\cdot\tilde{\mathbf{E}} - i\omega\mu_p\tilde{B}_\parallel\right)\hat{\Pi}F_0, \tag{21}$$

$$\frac{1}{M}\hat{\Pi} = \frac{\partial}{\partial\mathcal{E}} + \frac{cn}{e\omega}\frac{\partial}{\partial J}. \tag{22}$$

In Eq. (21) the terms describing the Larmor oscillations are omitted. However, the finite Larmor radius is taken into account: The term proportional $\tilde{B}_\parallel$ has arisen from $\overline{\mathbf{v}_L r_L^i}\partial\cdot\tilde{\mathbf{E}}/\partial r_{gc}^i = (-i\omega/\omega_B)(v_L^2)\tilde{B}_\parallel/(2c)$, where $\overline{(\ldots)} \equiv \oint d\alpha(\ldots)$ is averaging over Larmor rotation.

Now we integrate Eq. (21). Keeping only the terms responsible for the resonant wave-particle interaction, we have:

$$\tilde{F} = -\frac{1}{M}\hat{\Pi}F_0\int_{-\infty}^{t} d\tau\left(e\mathbf{v}_D\cdot\tilde{\mathbf{E}} - i\omega\mu_p\tilde{B}_\parallel\right), \tag{23}$$

Below we will show that due to the presence of the term proportional to $\tilde{B}_\parallel$, the integrand in Eq. (23) can be expressed through the vector product of two equilibrium quantities, the field line curvature $\boldsymbol{\kappa}$ and $\mathbf{b}$. With this purpose, we eliminate fast magnetoacoustic waves from the consideration by using the following equation:

$$\tilde{p} + \frac{1}{4\pi}B_0\tilde{B}_\parallel \approx 0, \tag{24}$$

where p is the plasma pressure. This equation implies that the Alfvén waves weakly disturb the total pressure of the plasma and the magnetic field, which was shown for stellarator plasmas in Ref.[18]. Then we assume that the plasma is incompressible, which leads to $\tilde{p} = -i\tilde{\mathbf{u}}_\perp\cdot\nabla p_0/\omega$ ($\tilde{\mathbf{u}}_\perp = cB_0^{-1}[\tilde{\mathbf{E}}\times\mathbf{b}]$ is the plasma hydrodynamic velocity) and obtain $\tilde{B}_\parallel$ from Eq. (24) as

$$\tilde{B}_\parallel = \frac{4\pi i}{\omega}\frac{c}{B_0^2}(\mathbf{b}\times\nabla p_0)\cdot\tilde{\mathbf{E}}. \tag{25}$$

Using Eq. (25) and $\mathbf{v}_D = \omega_B^{-1}\mathbf{b} \times \left(v_\parallel^2 \boldsymbol{\kappa} + \mu_p \nabla B_0/M\right)$, $\boldsymbol{\kappa} = B_0^{-2}\nabla_\perp(B_0^2/2 + 4\pi p_0)$, we obtain:

$$\overline{\mathbf{v}\cdot\tilde{\mathbf{E}}} = \mathbf{v}_D \cdot \tilde{\mathbf{E}} - ie^{-1}\omega\mu_p \tilde{B}_\parallel = \omega_B^{-1}(v_\parallel^2 + 0.5v_\perp^2)(\mathbf{b}\times\boldsymbol{\kappa})\cdot\tilde{\mathbf{E}}. \tag{26}$$

Now we put Eq. (26) into Eq. (23), which yields:

$$\tilde{F} = -\frac{e}{M}\hat{\Pi}F_0 \int_0^\infty dt'\, \omega_B^{-1}\left(v_\parallel^2 + 0.5v_\perp^2\right)[\mathbf{b}\times\boldsymbol{\kappa}(\tau)]\cdot\tilde{\mathbf{E}}(\tau)|_{\tau=t-t'}. \tag{27}$$

The energy exchange between the energetic ions and the waves is given by

$$\int d^3x\, \tilde{\mathbf{j}}\cdot\tilde{\mathbf{E}} = e\int d^3x\, d^3v\, \omega_B^{-1}(v_\parallel^2 + 0.5v_\perp^2)(\mathbf{b}\times\boldsymbol{\kappa})\cdot\tilde{\mathbf{E}}\,\tilde{F}. \tag{28}$$

When writing Eq. (28), we have taken $\tilde{\mathbf{j}} = e\int d^3v\,\mathbf{v}\tilde{F}$ and used the average value of $\mathbf{v}\cdot\tilde{\mathbf{E}}$ given by Eq. (26). We neglect the variation of the particle velocities during orbital motion. Then the spatially dependent part of the integrand in Eq. (28) can be presented as a product of $\tilde{F}$ and $\boldsymbol{\mathcal{K}}\cdot\tilde{\mathbf{E}}$ with $\boldsymbol{\mathcal{K}} \equiv (\mathbf{b}\times\boldsymbol{\kappa})/B$. We expand the quantities in this product into a Fourier series according to Eq. (1). Then the angle averaging enables us to write:

$$\int d^3x\,\tilde{F}(\boldsymbol{\mathcal{K}}\cdot\tilde{\mathbf{E}}) = \sum_{m,n}\int d^3x\, F_{m,n}(\boldsymbol{\mathcal{K}}\cdot\tilde{\mathbf{E}})^*_{m,n}. \tag{29}$$

To determine $(\boldsymbol{\mathcal{K}}\cdot\tilde{\mathbf{E}})_{m,n}$, we expand the field line curvature in a Fourier series as follows:

$$\boldsymbol{\mathcal{K}} = \sum_{p,s}\boldsymbol{\mathcal{K}}_{p,s}(r)e^{ip\vartheta + is\varphi}, \tag{30}$$

where p and s are integers. Then, using Eqs. (1) and (30), we find

$$(\boldsymbol{\mathcal{K}}\cdot\tilde{\mathbf{E}})_{m,n} = \sum_{p,s}\boldsymbol{\mathcal{K}}_{p,s}\cdot\mathbf{E}_{m-p,n+s}. \tag{31}$$

We have to specify the particle orbits in order to calculate $\tilde{F}_{m,n}$. As in Ref.[9], we neglect effects of the orbit width and assume that $\vartheta(\tau) = \vartheta + \omega_\vartheta\tau$ and $\varphi(\tau) = \varphi + \omega_\varphi\tau$, where $\omega_\vartheta = \text{const}$ and $\omega_\varphi = \text{const}$ are the frequencies of the poloidal and toroidal rotation, respectively. Then Eq. (27) yields:

$$F_{m,n} = c\left(v_\parallel^2 + 0.5v_\perp^2\right)\hat{\Pi}F_0\sum_{p,s}\frac{\boldsymbol{\mathcal{K}}_{p,s}\cdot\mathbf{E}_{m-p,n+s}}{i(\omega - m\omega_\vartheta + n\omega_\varphi)}. \tag{32}$$

Finally, combining Eqs. (17), (28), (31), and (32), we obtain the desired growth rate as follows:

$$\gamma_\alpha = 2\pi^2 M \frac{\sum_{m,n} \int dr\, r \int d^3v\, (v_\parallel^2 + 0.5 v_\perp^2)^2 \hat{\Pi} F_0 \sum_{p,s} |\boldsymbol{\mathcal{K}}_{p,s} \cdot \mathbf{E}_{m,n}|^2 \delta(\Omega_{mn}^{ps})}{\sum_{m,n} \int dr\, r \bar{v}_A^{-2} \left[|\Phi'_{m,n}|^2 + (m^2/r^2) |\Phi_{m,n}|^2 \right]}, \tag{33}$$

where

$$\Omega_{mn}^{ps} = \omega - (m+p)\omega_\vartheta + (n-s)\omega_\varphi, \tag{34}$$

and the velocity integral should be taken over the region corresponding to circulating particles.

The operator $\hat{\Pi}$ in the variables $\mathcal{E}$, μ_p and J is given by Eq. (22). When the particle energy well exceeds $\mathcal{E}_c \sim (M_i/M_e)^{1/3} T_e$, where T_e is the electron temperature, the Coulomb collisions change the particle magnetic moment, but $\lambda \equiv \mu_p \bar{B}/\mathcal{E}$ is weakly affected. Therefore, it is convenient to use λ instead of μ_p. In addition, because the orbit width of circulating particles is small, ψ can be used instead of J. Then $F_0 = F_0(\mathcal{E}, \lambda, \psi)$. In these variables, the velocity anisotropy gives rise to an additional term in $\hat{\Pi}$:

$$\hat{\Pi} = M \frac{\partial}{\partial \mathcal{E}} - \frac{M\lambda}{\mathcal{E}} \frac{\partial}{\partial \lambda} + \frac{n\bar{B}}{\omega \bar{\omega}_B \iota} \frac{\partial}{\partial \psi}. \tag{35}$$

The expression in the integrand of Eq. (33) can be simplified when $Nr^2/R^2 \ll 1$ and $N\beta \ll 1$, which is typically fulfilled in stellarators. In this case the terms proportional to $B_3(\psi)$ dominate $\boldsymbol{\mathcal{K}} \cdot \mathbf{E}$; therefore, $\boldsymbol{\mathcal{K}} \cdot \mathbf{E} \approx \kappa_1 E_2 - \kappa_2 E_1$, which leads to

$$|\boldsymbol{\mathcal{K}}_{p,s} \cdot \mathbf{E}_{m,n}|^2 \approx \frac{1}{r^2 \bar{B}^2} \left| i\kappa_{II} \frac{\partial \Phi_{m,n}}{\partial r} + m\kappa_I \Phi_{m,n} \right|^2, \tag{36}$$

where $\kappa_I \equiv \kappa_{r;p,s}$, $\kappa_{II} \equiv \kappa_{\vartheta;p,s}$, κ_r and κ_ϑ are covariant components of the p,s harmonics of the curvature.

The curvature harmonics can be expressed through the harmonics of the magnetic field strength, except for the harmonic $\kappa_{r;0,0}$. Therefore, it is convenient to write $\boldsymbol{\kappa}$ in a form that corresponds to B given by Eq. (2):

$$\boldsymbol{\kappa} = \frac{1}{2} \sum_{\mu,\nu=-\infty}^{\infty} \boldsymbol{\kappa}_{\mu,\nu} \exp(i\mu\vartheta - i\nu N\varphi). \tag{37}$$

On the other hand, the main Fourier harmonics of the magnetic field strength are proportional to $\cos(\mu\vartheta - \nu N\varphi)$, i.e., $\epsilon_B^{(\mu\nu)}$ in Eq. (2) are real and $\epsilon_B^{(\mu\nu)} = \epsilon_B^{(-\mu,-\nu)}$. In this case Eq. (2) is reduced to

$$B = \bar{B}[1 + \epsilon_0(r) + \sum_{\mu,\nu\neq 0} \epsilon_B^{(\mu\nu)}(r)\cos(\mu\vartheta - \nu N\varphi)], \tag{38}$$

where $\epsilon_0(r) = \epsilon^{(00)}/2$, and the sign of μ is fixed (we will assume $\mu > 0$). Then $\kappa_I = 0.5\sum_{\mu,\nu}\kappa_{r;\mu\nu}\delta_{\pm\mu,p}\delta_{\pm\nu N,-s}$, and $\kappa_{II} = 0.5i\sum_{\mu\nu}\mu\epsilon_B^{(\mu\nu)}\delta_{\pm\mu,p}\delta_{\pm\nu N,-s}$. Taking this into account and using Eq. (34), we can approximate the quantity $\sum_{ps}|\boldsymbol{\mathcal{K}}_{p,s}\cdot\mathbf{E}_{m,n}|^2\delta(\Omega_{m,n}^{p,s})$ in Eq. (33) as

$$\sum_{p,s}|\boldsymbol{\mathcal{K}}_{p,s}\cdot\mathbf{E}_{m,n}|^2\delta(\Omega_{mn}^{ps}) \approx \frac{1}{4r^2\bar{B}^2}\sum_{\mu,\nu,j}\left|j\mu\epsilon_B^{(\mu\nu)}\frac{\partial\Phi_{m,n}}{\partial r} - m\kappa_{r;\mu,\nu}\Phi_{m,n}\right|^2 \times \delta\left(\Omega_{m,n}^{p,s}\right)\Big|_{p=j\mu,\, s=-j\nu N}, \tag{39}$$

where $j = \pm 1$.

Let us consider the energetic ions consisting only of beam particles and characterized by very anisotropic pressure, $p_{b\parallel} \gg p_{b\perp}$, (the subscript "$b$" labels the beam particles), so that we can define β_b as $\beta_b = 8\pi p_{b\parallel}/B_0^2 = 8\pi M_b\int d^3v\, v_\parallel^2 F_0/B_0^2$. We assume that $F_0 = F_0(r, v, \chi)$ with $\chi^2 = 1 - \lambda \approx (v_\parallel/v)^2$. Then, basing on Eqs. (33)-(39), we can write the growth rate in a form convenient for the practical use as follows:

$$\gamma_b = \frac{\pi\beta_b(0)v_A^2(0)}{32a^2\omega\sum_{m,n}\int_0^1 d\rho\,\rho\left[|\Phi'_{m,n}|^2 + (m^2/\rho^2)|\Phi_{m,n}|^2\right]n_i(\rho)/n_i(0)} \times \sum_{m,n,\mu,\nu,j}\int_0^1\frac{d\rho}{\rho}\left|j\mu\epsilon_B^{(\mu\nu)}\Phi'_{m,n} - mk_{\rho;\mu,\nu}\Phi_{m,n}\right|^2\mathcal{Q}, \tag{40}$$

where $\rho = r/a$, a the plasma radius, $\Phi'_{m,n} = \partial\Phi_{m,n}/\partial\rho$, $\kappa_{\rho;\mu,\nu} = \partial\epsilon_B^{(\mu\nu)}/\partial\rho$ for $\mu \neq 0$, $\nu \neq 0$,

$$\mathcal{Q} = \left[2\int_0^\infty du\,u^4\int_{-1}^1 d\chi\,\chi^2 F_0(r=0,u,\chi)\right]^{-1} \times |w|\int_{|w|}^{|w|/\sqrt{\epsilon_{eff}}} du\,(u^2+w^2)^2\left[\frac{\partial}{\partial u} + \frac{(1-\chi_r^2)}{u\chi_r}\frac{\partial}{\partial\chi_r} + u\frac{\omega_{*b}}{\omega}\right]F_0(r,u,\chi_r), \tag{41}$$

$u = v/v_0$ with v_0 a characteristic velocity of injected ions, $w = v_\parallel^{res}(\rho)/v_0$, $v_\parallel^{res}(\rho) = \omega/(k_{mn} + 2jk^{\mu\nu})$, $\chi_r = w/u$ is the resonance pitch angle, $\omega_{*b} = nv_0^2(\omega_B\iota r)^{-1}\partial\ln(F_0)/\partial r$, ϵ_{eff} is determined from the condition that the particle trapping parameter equals unity.

For the parallel neutral injection in plasmas with a large aspect ratio, most energetic ions typically have pitch angles close to unity, in which case $\mathcal{Q}$ does not depend on ϵ_{eff}.

The term proportional to the pitch-angle derivative in Eq. (41) is minimum when $\chi_r^2 \to 1$, but it can play a considerable destabilizing role for smaller pitch angles. For instance, the drive produced by the velocity anisotropy overrides the damping caused by the negative velocity derivative ($\partial F_0/\partial v < 0$) when $F_0 \propto v^{-3}\delta(\chi - \chi_0)\eta(v_0 - v)$ ($\eta(x) = \int_{-\infty}^{x}\delta(y)dy$ is a step function) and $w < |\chi_0| < 0.77$.[20] More realistic beam distributions have weaker velocity dependence, which increases the interval of the particle pitch angles for which the anisotropy drive exceeds the damping. The effect is the largest for instabilities driven through the resonances involving the beam particles with velocities $v \ll v_0$. A simple example of a more realistic distribution is

$$F_0 = \frac{n_b(r)}{v^3 + v_c^3}\,\delta(\chi - \chi_0)\eta(v_0 - v), \tag{42}$$

where n_b is the beam density, $v_c = (1.33 M_e n_e^{-1}\sum_i n_i Z_i^2/M_i)^{1/3}\, v_{Te}$ with $v_{Te} = \sqrt{2T_e/M_e}$, Z_i is the charge number. Then we obtain for $|\chi_0| \neq 1$:

$$\mathcal{Q} = \frac{w^2}{I\chi_0^2(1 + u_c^3\chi_0^3/w^3)}\left\{\frac{\omega_{*b}}{\omega}\left(\frac{1}{\chi_0^2} + 1\right)^2 w^2 \right.$$
$$\left. + \frac{1}{(1 + u_c^3\chi_0^3/w^3)}\left[\frac{3}{\chi_0^4} - \frac{2}{\chi_0^2} - 5 + 2u_c^3\left(\frac{3}{\chi_0^2} + 2 - \chi_0^2\right)\frac{\chi_0}{w}\right]\right\}\frac{n_b(\rho)}{n_b(0)}, \tag{43}$$

where $|w| < 1$, $\chi_0 w > 0$, $u_c = v_c/v_0$, $I \equiv 2\int_0^1 du u^4/(u^3 + u_c^3)$, $I \approx 1$ for $u_c^3 \ll 1$. When $|w| > 1$ or $\chi_0 w < 0$, $\mathcal{Q} = 0$ because in this case the resonant particles are absent. We observe that the second term proportional to u_c^3 is destabilizing, as expected.

For the special case of $\chi_0 = 1$ we get:

$$\mathcal{Q} = \frac{4w^2}{I(1 + u_c^3/w^3)}\left(\frac{\omega_{*b}}{\omega}w^2 - \frac{2 - u_c^3/w^3}{1 + u_c^3/w^3}\right)\frac{n_b(\rho)}{n_b(0)}. \tag{44}$$

Note that when a mode consists of a pair of Fourier harmonics equally contributing to the denominator of Eq. (40), and both harmonics are strongly localized, Eq. (40) for the growth rate is reduced to

$$\gamma_{local} = \frac{\pi\beta_b v_A^2}{64 r^2\omega}\sum_{j,\mu,\nu}\mu^2|\epsilon_B^{(\mu\nu)}|^2\mathcal{Q}. \tag{45}$$

IV. NUMERICAL SIMULATION OF ALFVÉN INSTABILITIES IN A PARTICULAR LHD SHOT

A. Experimental data, equilibrium characteristics, and Alfvén continuum

In this section we consider low-mode-number Alfvén instabilities observed during Neutral Beam Injection (NBI) in the LHD shot #24512. We concentrate on the instabilities with the frequencies in the range of $50 - 80$ kHz and the mode numbers $|n| = 1, 2$ and $|m| = 2, 3$, see Fig. 4. These instabilities were first reported in Refs.[15,17]. In the mentioned works, a detailed description of the observations was presented, and the Alfvén continua were calculated. It was found that the frequencies of the observed modes correspond to the region of the TAE gap. On this ground, the instabilities were identified as TAE instabilities. In addition, a guess was made through careful comparison with experimental observations[2,21] in CHS (Compact Helical System[22]) that the observed $n = 1$ modes were core-localized even and odd TAEs, whereas the $n = 2$ modes were global TAEs, although no eigenmode calculations were carried out. In this work, we further investigate the instabilities: We solve the eigenvalue problem, analyze the mode interaction with the energetic ions, and calculate the growth rates of the instabilities.

The instabilities were driven by ions produced by NBI. Hydrogen ions were injected tangentially with the particle energy $\mathcal{E}_0 \approx 150\,\mathrm{keV}$ into a helium plasma. The major radius of the torus in the mentioned experiment was $R_0 = 3.6\,\mathrm{m}$, which was favourable for the confinement of various groups of the particles.[23] Equilibrium parameters, such as the electron density, temperature, and the rotational transform, at the moment $t = 1.8\,\mathrm{s}$ (when the instabilities were observed) are shown in Fig. 5. In these figures, in addition, β ($\beta = 8\pi p_0/B_0^2$) and β_b are presented. It follows from Fig. 5 that the beam ion pressure was very large; it exceeded the plasma pressure in the near-axis region. In addition, it was very peaked. The shown equilibrium characteristics were calculated with the code described in Refs.[24,25]. The finite particle orbit width and possible diffusion of fast ions were neglected in the calculation of β_b. Therefore, one can expect that in reality the pressure profile of the energetic ions will be somewhat wider and the central β_b somewhat lower. Figure 5

shows, in addition, the beam velocity distribution calculated with the same code. We can conclude from here that (i) the beam consists only from the well circulating particles, and (ii) the most energetic ions are located in the plasma core; therefore, the beam can hardly lead to edge-localized instabilities.

In order to calculate AC, we need Fourier harmonics of the equilibrium magnetic field and the metric tensor component $g^{\psi\psi}$. The dominant harmonics of these magnitudes are shown in Fig. 6. We observe that $\epsilon_g^{(21)}$ is very large at the periphery, which leads to a very wide HAE_{21} gap in AC and strongly shifts down all the gaps at the plasma periphery, see Fig. 7. On the other hand, the average TAE gap frequency [the gap is rather narrow, $\Delta_\omega \ll \omega_*$ with ω_* given by Eq. (4)] grows with the radius even at the periphery [although it is not proportional to ι, as predicted by Eq. (4)]. In addition, we observe that the characteristic frequencies determined simply by crossing two cylindrical branches of AC lie inside the gap for $r/a < 0.55$. Therefore, we conclude that the toroidal coupling (i.e., coupling with $\nu \neq 0$) has a considerable influence only on those TAE modes which are localized close to the plasma edge (but it is not clear whether such modes exist).

The continuum shown in Fig. 7 is calculated by the code COBRA (COntinuum BRanches of Alfvén waves).[6] It was assumed that the helium plasma is homogeneous and has $n_i = 5 \times 10^{12}\mathrm{cm}^{-3}$. The latter, as it follows from Fig. 5, can be considered as a characteristic density when $n_i = n_e/2$. Below we assume that the plasma consists only of helium (i.e. we neglect the effect of the injected hydrogen and impurities on the Alfvén velocity). Then the picture of AC taking into account the spatial inhomogeneity of the plasma can be easily obtained from that presented in Fig. 7 by multiplying the shown AC by $\sqrt{10^{13}/n_e(r)}$ with $n_e(r)$ given by Fig. 5.

The considered non-monotonic profile of the plasma density with $n_e(r)$ having a maximum at $r/a \approx 0.6$ is a favourable factor for minimizing the continuum damping in the region $r/a \lesssim 0.6$ (it "helps" to avoid the crossing of the AC in the plasma core with the horizontal line representing a TAE eigenfrequency). Therefore, core-localized AEs have more chances to exist a realistic plasma than in a plasma with homogeneous density. However, this effect competes with the increase of the TAE gap frequency caused by the

$\iota(r)$ increase. Therefore, only a direct calculation of the radial structure of AE can give an answer to the question of whether core-localized TAE modes do exist.

B. Eigenmode analysis and the calculation of growth rates of the instabilities

Although the knowledge of AC is important, the calculation of AC is only the first step on the way to the identification of the observed instabilities. The next step is to clarify whether Alfvén eigenmodes exist. If they exist, we have to compare the calculated eigenfrequencies and the mode numbers with experimental data. With this purpose we use the following ideal MHD equations:[6]

$$\begin{aligned}
&\frac{\partial}{\partial r} r^3 \left(\frac{\omega^2}{\bar{v}_A^2} - k_{m,n}^2 \right) \frac{\partial E_{m,n}}{\partial r} + Q_{m,n} E_{m,n} \\
&+ \sum_{\mu,\nu} \frac{\partial}{\partial r} r^3 \left[\frac{\omega^2}{\bar{v}_A^2} \left(\frac{\epsilon_g^{(\mu\nu)}}{2} - 2\epsilon_B^{(\mu\nu)} \right) - k_{m,n} k_{m+\mu,n+\nu N} \frac{\epsilon_g^{(\mu\nu)}}{2} \right] \frac{\partial E_{m+\mu,n+\nu N}}{\partial r} \\
&+ \sum_{\mu,\nu} \frac{\partial}{\partial r} r^3 \left[\frac{\omega^2}{\bar{v}_A^2} \left(\frac{\epsilon_g^{(\mu\nu)}}{2} - 2\epsilon_B^{(\mu\nu)} \right) - k_{m,n} k_{m-\mu,n-\nu N} \frac{\epsilon_g^{(\mu\nu)}}{2} \right] \frac{\partial E_{m-\mu,n-\nu N}}{\partial r} = 0,
\end{aligned} \tag{46}$$

where $E_{m,n} = \Phi_{m,n}/r$,

$$Q_{m,n} = r \left(\frac{\omega^2}{\bar{v}_A^2} - k_{m,n}^2 \right) (1 - m^2) + r^2 \frac{d}{dr} \left(\frac{\omega^2}{\bar{v}_A^2} \right). \tag{47}$$

Equation (46) is actually an infinite set of second-order equations for the wave amplitudes. However, as follows from the above analysis of AC, the toroidal coupling plays a minor role for the TAE modes of interest. For this reason, we neglect it. In addition, using Fig. 2, Fig. 7 and the analysis in Sec. 2, we conclude that a TAE mode in the considered case (if it exists) consists of only few harmonics. This conclusion agrees with the experimental data where the poloidal mode number for the $|n| = 1$ instability was determined to be $|m| = 2$, whereas the poloidal mode number $|m| = 3$ was determined for the $|n| = 2$ instability. Therefore, it seems reasonable to restrict ourselves to four equations coupled by $\epsilon_B^{(10)}$ and $\epsilon_g^{(10)}$. To solve these equations, we use the code BOA (Branches Of Alfvén modes).[6]

We should note the following. The equation for the ideal-MHD Alfvén waves has a singularity at the point of the local Alfvén resonance, r_{res} (determined by the equation

$\omega = \omega_A(r_{res})$, where $\omega_A(r)$ is a continuum branch). Therefore, strictly speaking, it has solutions only for completely open gaps in AC, when such a resonance is absent (the problem of existence of Alfvén eigenmodes in an inhomogeneous plasma was considered in, e.g., Ref.[26]). Nevertheless, when the resonance is located in the "tail" of the eigenfunction, i.e., at a radius where the mode amplitude is much less than its maximum magnitude, this resonance has only a minor influence on the solution. One can say that in this case the AE exists. In other words, the continuum damping rate is small when the resonance point is located far in the tail of the radial distribution of the amplitude. When the ideal MHD equations are solved numerically, a sharp maximum appears at the point of the local Alfvén resonance. Therefore, a problem of selecting weakly damped modes arises. In order to solve this problem without a special calculation of the continuum damping, one should change the mesh. Then the "good" solutions representing weakly damped modes will persist, whereas the damped solutions will disappear and new damped solutions appear.

Assuming that the dependence of perturbations on the angular coordinates is given by Eq. (1)), we consider the modes with $m, n < 0$ because only they can be destabilized by the spatial inhomogeneity of the beam ions, see Eq. (40). Note that the modes with positive mode numbers can be destabilized when the velocity anisotropy of the beam ions is the main driving factor. However, the considered shot was characterized by the large pressure gradient of the beam ions, $\omega_{*b} \gg \omega$; therefore, the velocity anisotropy played a minor role. One can see that when $n < 0$, the mode rotates in the clockwise direction, which agrees with the experiment.[17]

We have made calculations for both $n = -1$ and $n = -2$ modes observed experimentally. The solutions showing the existence of two TAE modes with $n = -1$ (which we refer to as the $n = 1$ mode) were obtained. However, no discrete modes with $n = -2$ were found in the framework of the used equilibrium and the used equations. The calculated $n = -1$ modes are localized around the radius $r/a \sim 1/3$ and have the dominant modes numbers $m = -2, -3$. Their eigenfrequencies and the radial structures are shown in Fig. 8. These eigensolutions were obtained for various meshes, the number of points varying from 100 to 500. Therefore, the obtained solutions indeed describe discrete modes. We observe

that the TAE mode with lower ω consists of harmonics with different phases (i.e., this is an "even" TAE), whereas the higher mode consists of harmonics with the same phase (an "odd" TAE). This result confirms the guess made in Ref.[17]. Furthermore, the ratio of frequencies of these modes agrees with the experimental data. Note that the code calculates normalized frequencies, $\tilde{\omega} = \omega R_0/\bar{v}_A$. If we assume that the plasma consisted only of helium, we obtain that the calculated frequencies are somewhat less than those observed experimentally. On the other hand, considering a hydrogen plasma we obtain the frequencies exceeding the experimental magnitudes (the ratio of Alfvén velocity in a hydrogen plasma to that in a helium plasma is $\sqrt{2}$). The best agreement between the calculated frequencies and the experimental frequencies is reached for a plasma consisting of a mixture of helium and hydrogen, which was the case in the experiment: A simple estimate shows that the fraction of hydrogen in the core was rather large. In order to make this estimate, one should take into account that two hydrogen beams with the total power 3MW were injected for $\Delta t \sim 1.5\,\mathrm{s}$ before the instability and that the slowing down time of beam ions was much less than Δt, which resulted in the production of a so significant number of thermal protons that their density would exceed the helium density unless the hydrogen diffusion were strong. Moreover, a numerical simulation with the code[24,25] shows that even the partly-thermalized hydrogen ions constitute a considerable fraction of the plasma ions in the plasma core.

Now we proceed to a study of the destabilization of the $n = 1$ even and odd TAE modes by the beam ions. Because each mode consists only of a pair of the dominant Fourier harmonics, we can use Fig. 3 showing the resonant velocities for this case. It follows from Fig. 3 that the modes are affected by the energetic ions only through the toroidicity-induced resonance. Another conclusion is that $|v_\parallel^{res}| \approx v_A/3$, which is considerably less than the beam velocity v_0. However, Fig. 3 ignores the finite radial width of the mode, Δr_{mode}. Because v_0 is only a little bit less than v_A, the finite magnitude of Δr_{mode} can provide the interaction between the modes and the particles with $\mathcal{E} \lesssim 150keV$, as was shown in Sec. II B [see Eq. (15) and a discussion after it]. In order to clarify whether this is indeed the case, we have calculated the resonant velocities in the region where the

modes are localized, see Fig. 9. We observe that $|w| \sim 1$ at $r/a \sim 0.32$ for the even mode and $r/a \sim 0.36$ for the odd mode. Because the even mode amplitude is considerable and its radial derivative is large at $r/a \sim 0.32$, one can expect that the finite radial width of the mode will strongly enhance the growth rate [by a factor of $(3v_0/v_A)^4$ because, roughly speaking, $\gamma_b \propto w^4$]. The enhancement of the growth rate of the odd mode should be much weaker because for this mode both the mode amplitude and its derivative are much less in the region where $|w| \sim 1$. Direct calculations based on the use of Eqs. (40), (43) have confirmed these conclusion. It was found that $\gamma_b/\omega \approx 20\beta_b(0)$ for the even mode and $\gamma_b/\omega \approx 2\beta_b(0)$ for the odd mode.

In the calculations we took the beam density distribution in the following two forms: $n_b(r) \propto (1-r^2/a^2)^2$ and $n_b(r) \propto \exp[-(r-r_0)^2/L_b^2]$ with $L_b = 0.5a$, $r_0 = 0.17a$, $a = 70\,\mathrm{cm}$. Both these expressions resulted in the same growth rate. They describe density profiles peaked less than those shown in Fig. 5. These distributions were chosen because the experimentally observed $n = 2$ instability with the frequency about 80 kHz indicates that $n_b(r)$ was more broad than that shown in Fig. 5. The matter is that the mentioned instability was, probably, localized at $r/a \sim 0.6$ (this follows from the fact that the $n = 2$ TAE gap with the frequencies $\sim 80\,\mathrm{kHz}$ is located at $r/a \sim 0.6$, see Fig. 2), which is hardly consistent with Fig. 5, where $d\beta/dr|_{r=0.6a} \ll d\beta/dr|_{r=0.3a}$. This implies that there is a mechanism leading to some broadening of $n_b(r)$, which was not taken into account in the calculation of $n_b(r)$. On the other hand, the energies of all the resonant particles, including the particles interacting with the modes through the $|v_\parallel| = v_A/3$ resonance, exceed the energy $\mathcal{E}_c$; thus, all the resonant particles were well anisotropic (see Fig. 5), which justifies the use of Eq. (43).

V. SUMMARY AND CONCLUSIONS

The work carried out contributes to the general theory of fast-ion-driven Alfvén instabilities in helical plasmas and contains specific examples and calculations relevant, first of all, to LHD. The results of the work can be summarized as follows.

We have shown that "conventional" resonances, i.e., the same resonances that exist

in tokamaks, determine the interaction of the energetic ions and low-frequency modes in LHD plasmas (e.g., TAE modes). On the other hand, "non-axisymmetric" resonances[9] are important for the high-frequency modes (various HAE modes and TAEs), especially, for the modes localized in the plasma periphery.

It is predicted that finite radial width of an Alfvén mode can strongly enhance the instability providing the interaction of the mode and most energetic particles in the case when such an interaction is not possible in the local approximation.

Because of a significant shear, the gaps in the low-frequency part of AC of LHD plasmas (in particular, the TAE gap) are characterized by a multi-harmonic structure, like in tokamaks. With such a structure of the gap, the multiple-harmonic TAE modes ("global" TAEs) usually exist in tokamaks with monotonic safety factor profiles. In contrast to tokamaks, the shear in LHD and other stellarators is usually negative. For this reason, AEs residing in such gaps typically consist only of a pair of dominant harmonics.

This conclusion, drawn from a qualitative consideration, was confirmed by numerical calculations carried out for the LHD shot #24512. In the mentioned shot an Alfvénic activity was observed with the frequencies in the range of $50 - 80$ kHz during tangential NBI.[16,17] The eigenmode calculations carried out with the BOA code[6] have shown that there are two discrete $n = 1$ TAE modes, the ratio of their frequencies being 1.2, which agrees with the experimental data. The magnitudes of the calculated frequencies (but not their ratio) depend on the composition of the plasma. In the considered shot a hydrogen beam was injected into a helium plasma. According to the estimates made, the fraction of hydrogen was significant in the plasma core. The assumption that the hydrogen fraction was about the helium fraction leads to the frequencies corresponding to the experiment. The lower calculated mode represents the "even" TAE, and the "upper" mode is the "odd" one, as in tokamaks, which corresponds to a guess made in Ref.[17]. Note that the "odd" mode was observed only recently in tokamaks, in experiments on JET (Joint European Torus[27]).[28]

The obtained radial structure of the $n = 1$ TAE modes enabled us to calculate the growth rate of the instabilities driven by energetic ions. It was found that the growth

rate of the even mode instability exceeds that of the odd mode by a factor of 10. The enhancement is associated with the finite radial width of the mode, which "switches on" the interaction of the mode and the particles with $\mathcal{E} \lesssim 150\,\mathrm{keV}$.

The growth rate of the mentioned $n = 1$ instability was calculated with the use of a general expression obtained in the work. This expression takes into account the finite magnitude of the perturbed longitudinal magnetic field (thus, it generalizes a corresponding expression of Ref.[9]) and has a form convenient for direct calculations.

Note that we have not calculated the mode damping rate, which should be done in order to obtain the threshold density of the energetic ions.

In addition to the described $n = 1$ mode, an $n = 2$ mode was observed in the same LHD shot. However, we failed to find discrete eigenmodes with $|n| = 2$ in the TAE gap. This may mean that the equilibrium model we used is not sufficiently good at the plasma periphery. A crucial factor, which affects the existence of TAE modes with the mode numbers $|n| = 2$, $|m| = 3$ and 4, is the radial dependence of $\iota(r)$ at $r/a \gtrsim 0.5$. Smaller shear in this region would facilitate the existence of the eigenmode.

ACKNOWLEDGMENTS

One of the authors (Ya.K.) acknowledges the hospitality of the National Institute for Fusion Science, Toki, where he was staying for three months as a Guest Professor.

REFERENCES

[1] King-Lap Wong, Plasma Phys. Control. Fusion **41**, R1 (1999).

[2] K. Toi, M. Takechi, M. Isobe *et al.*, Nucl. Fusion **40**, 1349 (2000).

[3] A. Weller, M. Anton, J. Geiger *et al.*, Phys. Plasmas **8**, 931 (2001).

[4] N. Nakajima, C. Z. Cheng, and M. Okamoto, Phys. Fluids B **4**, 1115 (1992).

[5] C. Nührenberg, Plasma Phys. Control. Fusion **41**, 1055 (1999).

[6] Ya. I. Kolesnichenko, V. V. Lutsenko, H. Wobig, Yu. V. Yakovenko, and O. P. Fesenyuk, *Alfvén Eigenmodes in Helias Configurations (Part I), IPP Report III/261* (Max-Planck-Institut für Plasmaphysik, Garching bei München, 2000); Phys. Plasmas **8**, 491 (2001).

[7] C. Nührenberg, in *ISSP-19 "Piero Caldirola", Theory of Fusion Plasmas*, edited by J. W. Connor, O. Sauter, and E. Sindoni (Editrice Compositori – Società Italiana di Fisica, Bologna, 2000), p. 313.

[8] M. Fujiwara, K. Kawahata, N. Ohyabu *et al.*, Nucl. Fusion **41**, 1355 (2001).

[9] Ya.I. Kolesnichenko, V.V. Lutsenko, H. Wobig, and Yu.V. Yakovenko, Phys. Plasmas **9**, 517 (2002).

[10] Ya. I. Kolesnichenko, V. V. Lutsenko, H. Wobig, and Yu.V. Yakovenko, Nucl. Fusion **42**, 949 (2002).

[11] C. D. Beidler, E. Harmeyer, F. Herrnegger *et al.*, Nucl. Fusion **41**, 1759 (2001).

[12] F. Wagner, Transactions of Fusion Technology **33**, 67 (1998).

[13] Ya. I. Kolesnichenko, V. V. Lutsenko, H. Wobig, and Yu. V. Yakovenko, *Alfvén Eigenmodes in Helias Configurations (Part II), IPP Report III/271* (Max-Planck-Institut für Plasmaphysik, Garching bei München, 2002).

[14] S. Yamamoto, K. Toi, S. Ohdachi *et al.*, in *29th European Physical Society Conference on Controlled Fusion and Plasma Physics, Montreux, 2002*, Europhysics Conference Abstracts (The European Physical Society, Petit-Lancy, 2002), Vol. 26B, Rep. P1-079.

[15] K. Toi, S. Ohdachi, S. Yamamoto, N. Nakajima *et al.*, "MHD instabilities and their effects on plasma confinement in the Large Helical Device plasmas", 19th International Atomic Energy Agency Fusion Energy Conference, Lyon (2002), Report IAEA-CN-94/EX/S3-2, to be published; Research Report NIFS-758 (2002).

[16] V. V. Lutsenko, Ya. I. Kolesnichenko, A. Weller, A. Werner, H.Wobig, Yu. V. Yakovenko, and O. P. Fesenyuk, "Peculiarities of destabilization of Alfvén modes by energetic ions in stellarators", ibid., Report IAEA-CN-94/TH/P3-16.

[17] S. Yamamoto, K. Toi, S. Ohdachi *et al.*, "Experimental studies of energetic-ion-driven MHD instabilities and their effects on energetic ion transport in the Large Helical Device plasmas", submitted to Nucl. Fusion.

[18] O. P. Fesenyuk, Ya. I. Kolesnichenko, H. Wobig, and Yu. V. Yakovenko, Phys. Plasmas **9**, 1589 (2002).

[19] C. D. Beidler, Ya. I. Kolesnichenko, V. S. Marchenko, I. N. Sidorenko, and H. Wobig, Phys. Plasmas **8**, 2731 (2001).

[20] V. S. Belikov, Ya. I. Kolesnichenko, and O. A. Silivra, Nucl. Fusion **32**, 1399 (1992).

[21] M. Takechi, K. Toi, S. Takagi *et al.*, Phys. Rev. Lett. **83**, 312 (1999).

[22] K. Matsuoka, S. Kubo, M. Hosokawa *et al.*, in *Plasma Physics and Controlled Nuclear Fusion Research 1988, 12th Conerence Proceedings, Nice, 1988* (International Atomic Energy Agency, Vienna, 1989), Vol. 2, p. 411.

[23] S. Murakami, H. Yamada, A. Wakasa *et al.*, "A demonstration of magnetic field optimization in LHD", 19th International Atomic Energy Agency Fusion Energy Conference, Lyon (2002), Report IAEA-CN-94/EX/C5-3, to be published; Research Report NIFS-750 (2002).

[24] K. Yamazaki and T. Amano, Nucl. Fusion **32**, 633 (1992).

[25] K. Yamazaki, N. Nakajima, S. Murakami, M. Yokoyama, and the LHD Group, J. Plasma Fusion Res. SERIES **2**, 125 (1999).

[26] A. V. Timofeev, in *Reviews of Plasma Physics*, Vol. 9 (Consultants Bureau, New York – London, 1986), p. 265.

[27] P. H. Rebut, R. J. Bickerton, and B. E. Keen, Nucl. Fusion **25**, 1011 (1985).

[28] G. J. Kramer, S. E. Sharapov, R. Nazikian, N. N. Gorelenkov, R. Budny, and contributors to the JET-EFDA Workprogramme, *First evidence for the existence of odd Toroidal Alfvén Eigenmodes (TAEs) from the simultaneous observation of even and odd TAEs on the Joint European Torus, Report PPPL-3768* (http://www.pppl.gov, Princeton Plasma Physics Laboratory, Princeton, 2003).

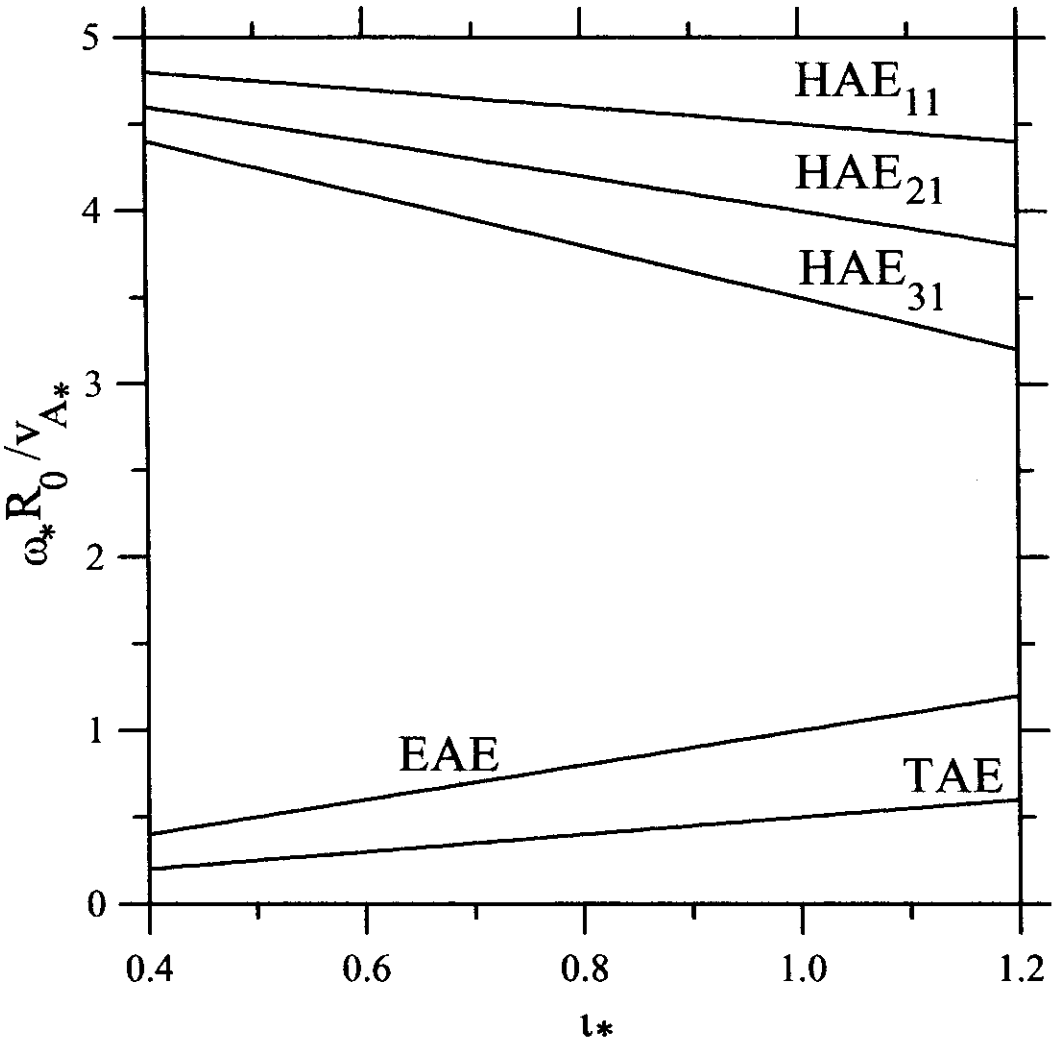

FIG. 1. Characteristic frequencies of gap modes in LHD determined by Eq. (4). Notations: subscripts at "HAE" denote the mode coupling numbers, μ and ν.

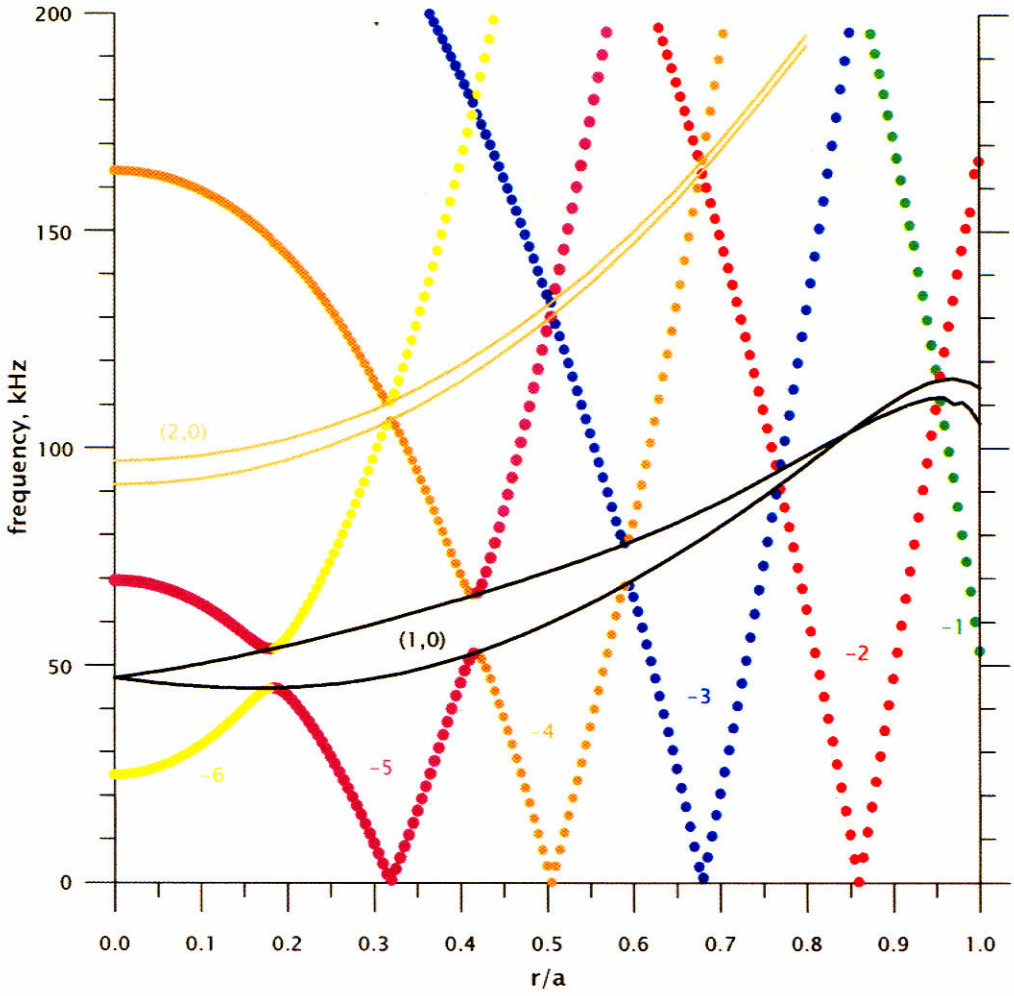

FIG. 2. Low-frequency part of Alfvén continuum for $n = -2$ family modes (i.e., only modes coupled with the $n = -2$ mode are taken into account) of the LHD shot #24512 but for constant ion density, $n_i(r) = 5 \times 10^{12}\,\mathrm{cm}^{-3}$. Two gaps in AC are clearly seen: TAE, $(1,0)$, and EAE, $(2,0)$. The numbers -1, -2, ... below the TAE gap denote the poloidal mode numbers.

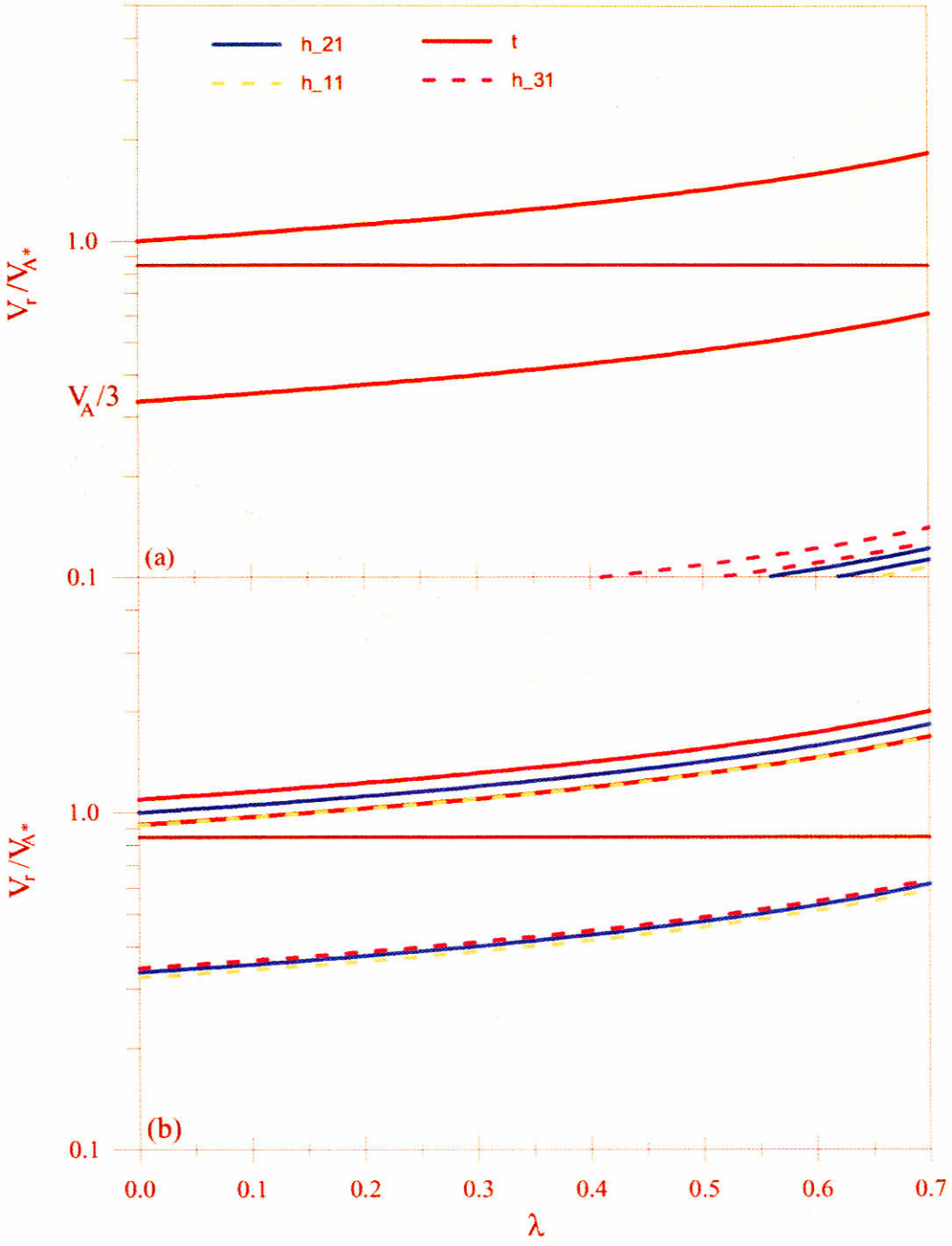

FIG. 3. Resonant velocities, $v_r = |v_\parallel^{res}|/(1-\lambda)^{1/2}$, described by Eq. (14) with $k^{\mu\nu}(r_0) = k^{\mu\nu}(r_s)$ versus the pitch-angle parameter $\lambda = \mu_p B_0/\mathcal{E}$ for the toroidal and three helical Fourier harmonics of the magnetic field strength in LHD: (a), for TAE modes; (b), for HAE_{21} modes.

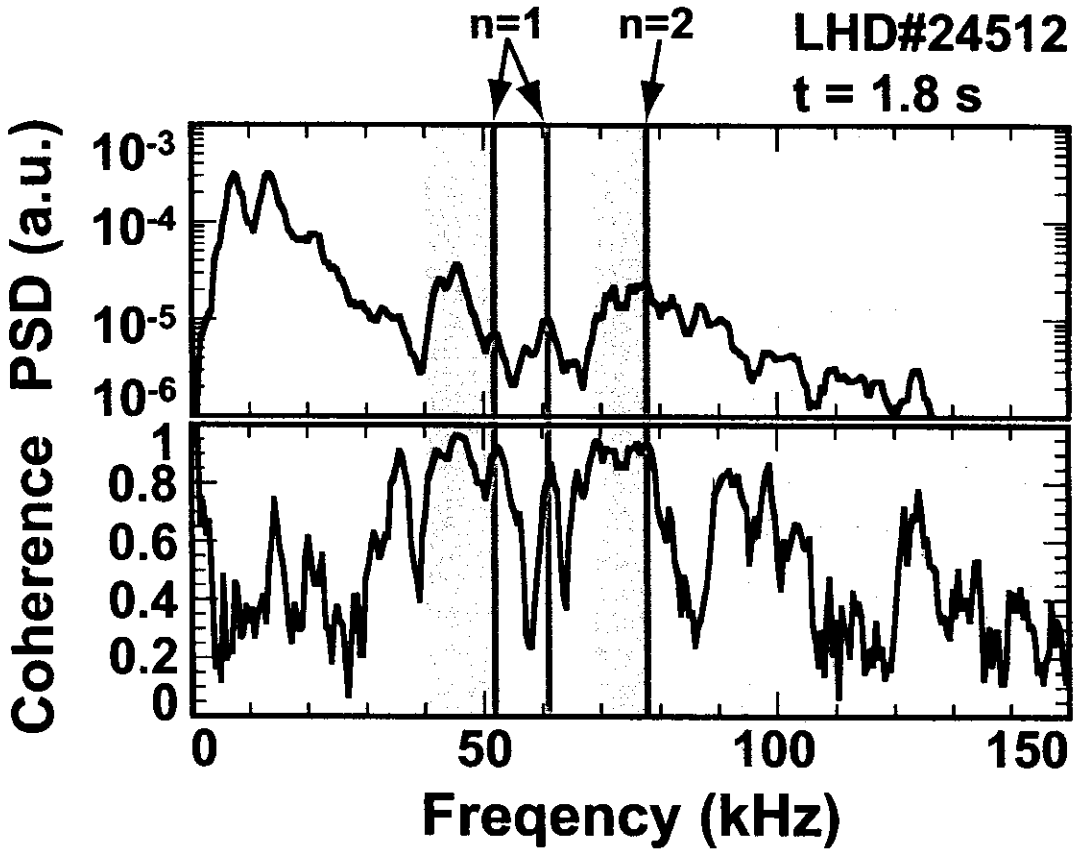

FIG. 4. Power spectrum of magnetic fluctuations in the LHD shot #24512 at $t = 1.8\,\mathrm{s}$.[17]

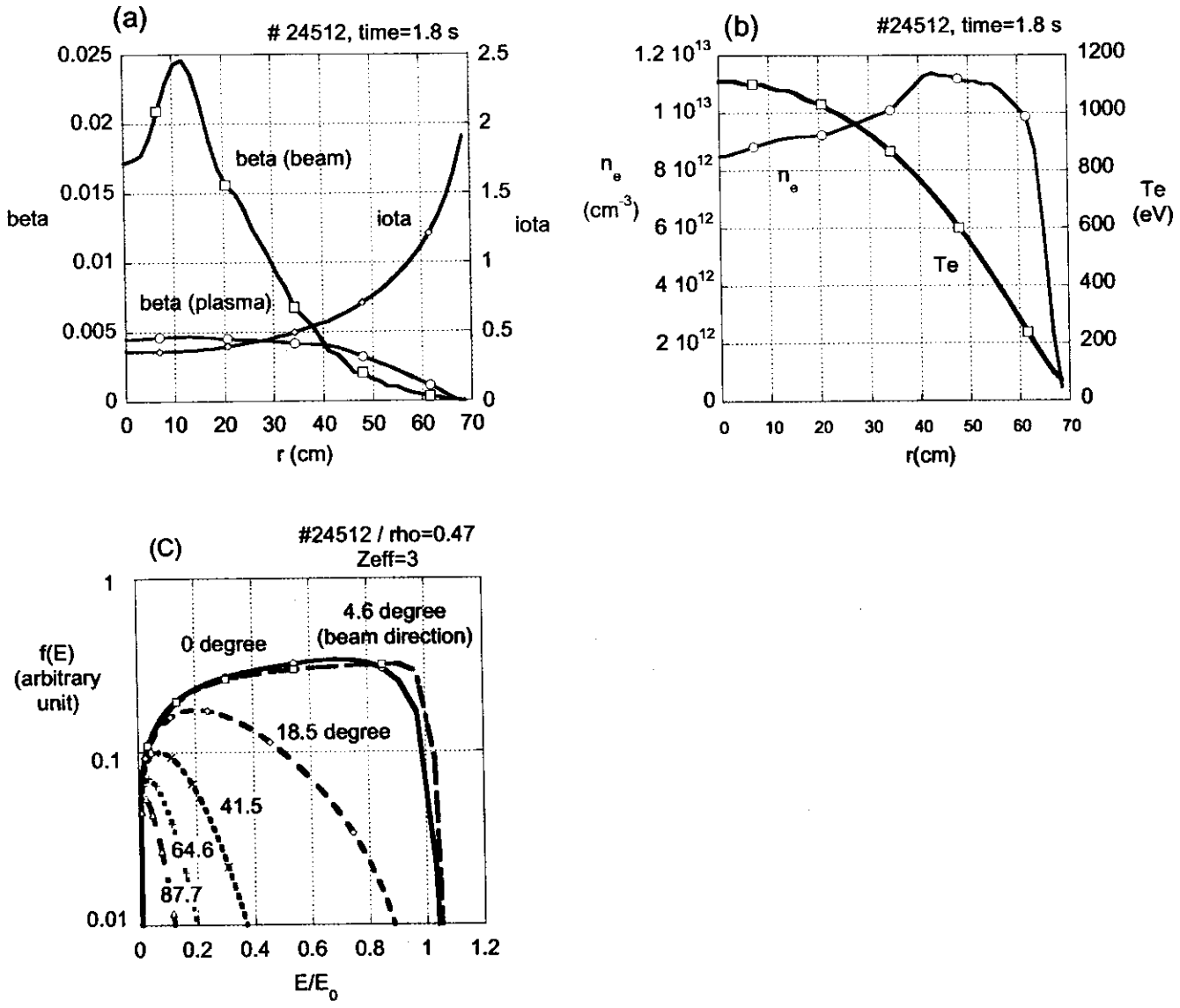

FIG. 5. Calculated equilibrium parameters versus radius in the LHD shot #24512 at $t = 1.8$ s: (a), the rotational transform, β and β_b; (b), the electron density and temperature; (c), the distribution function of the beam ions.

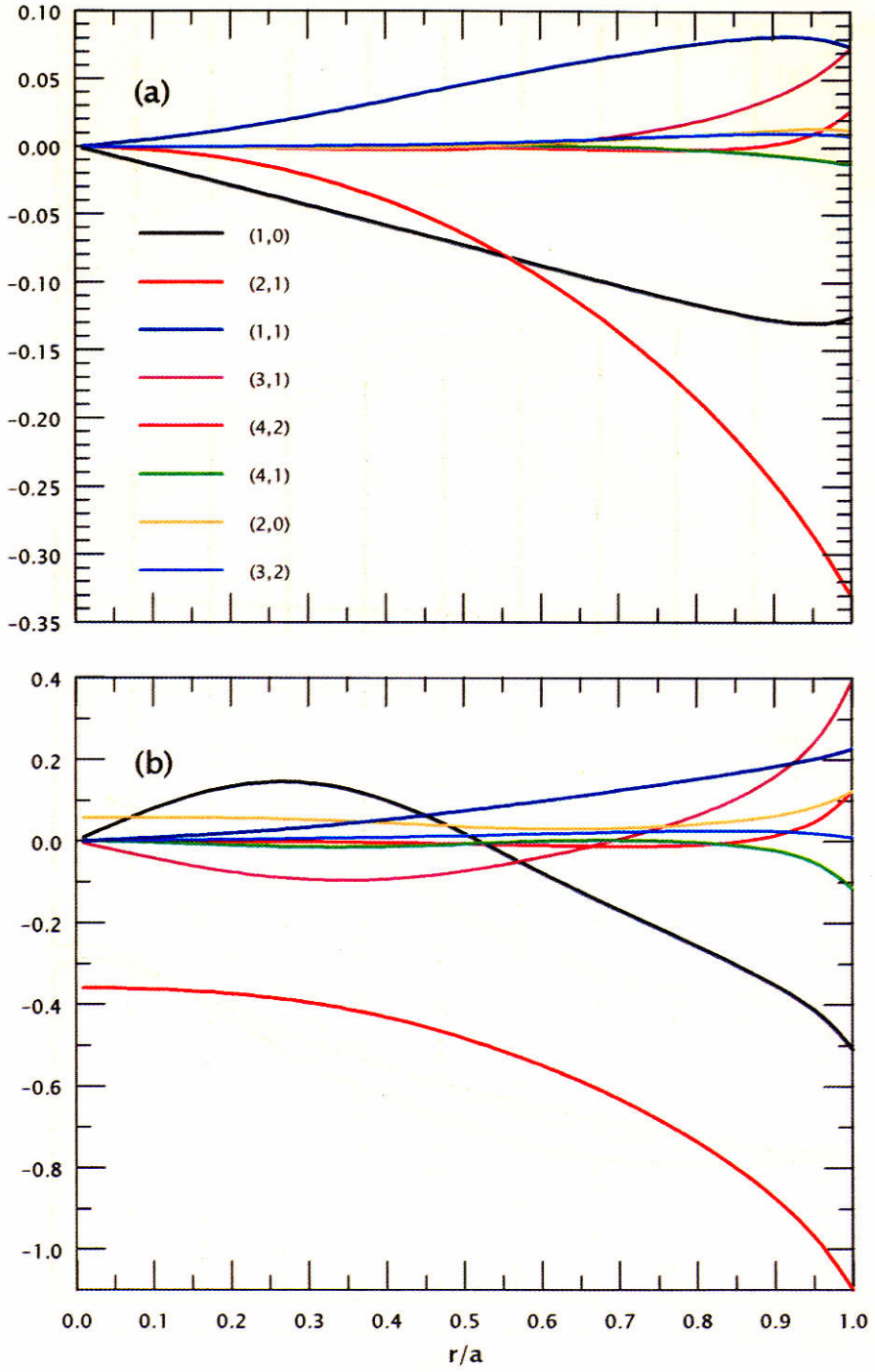

FIG. 6. Fourier harmonics of the magnetic field strength (a) and contravariant components of the metric tensor (b) in the LHD shot #24512.

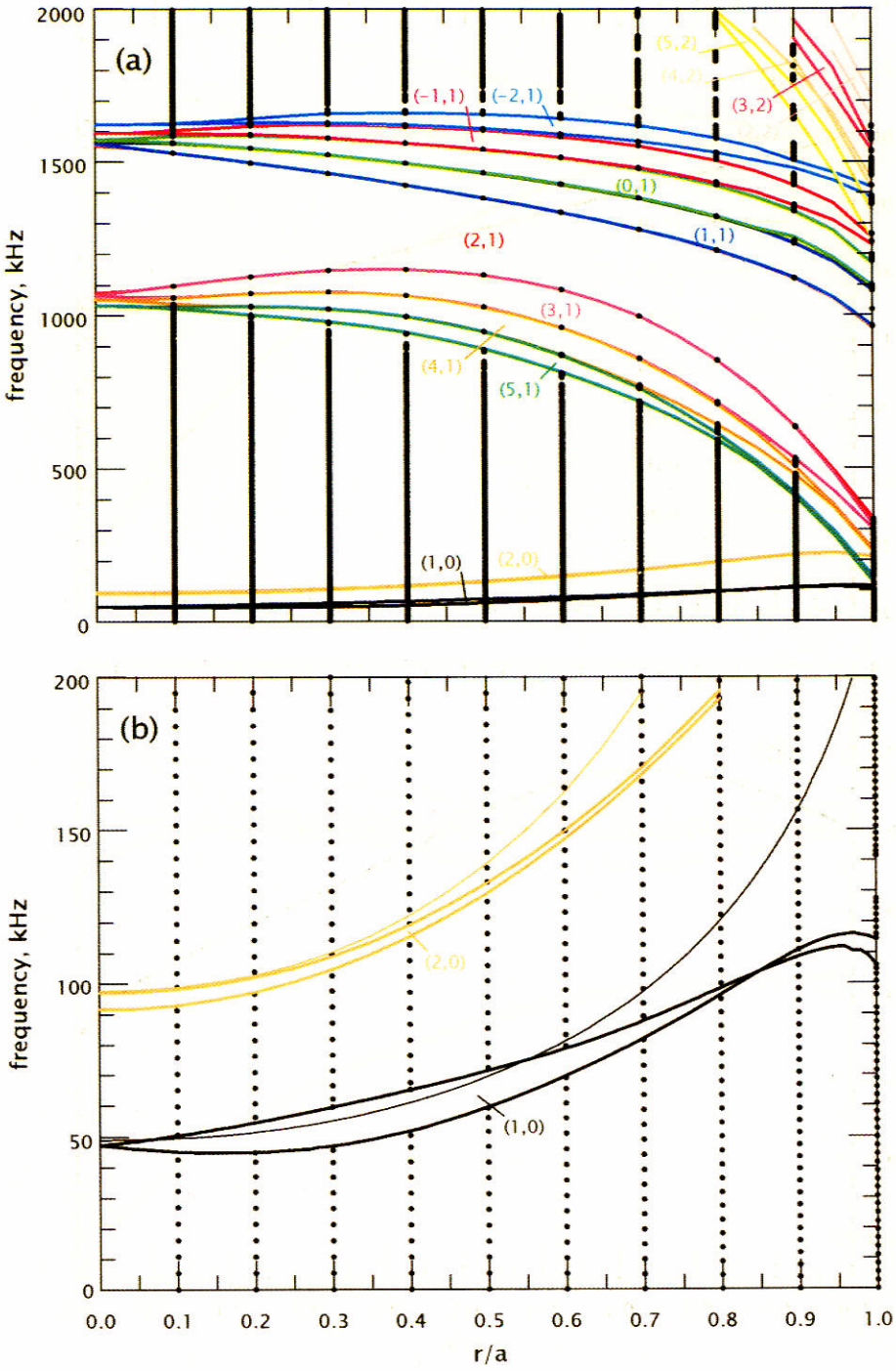

FIG. 7. Alfvén continuum (a) and its low-frequency part (b) of the LHD shot #24512 but for $n_i(r) = 5 \times 10^{12}\,\mathrm{cm}^{-3}$. The dotted line inside the TAE gap shows the TAE characteristic frequency determined by Eq. (4).

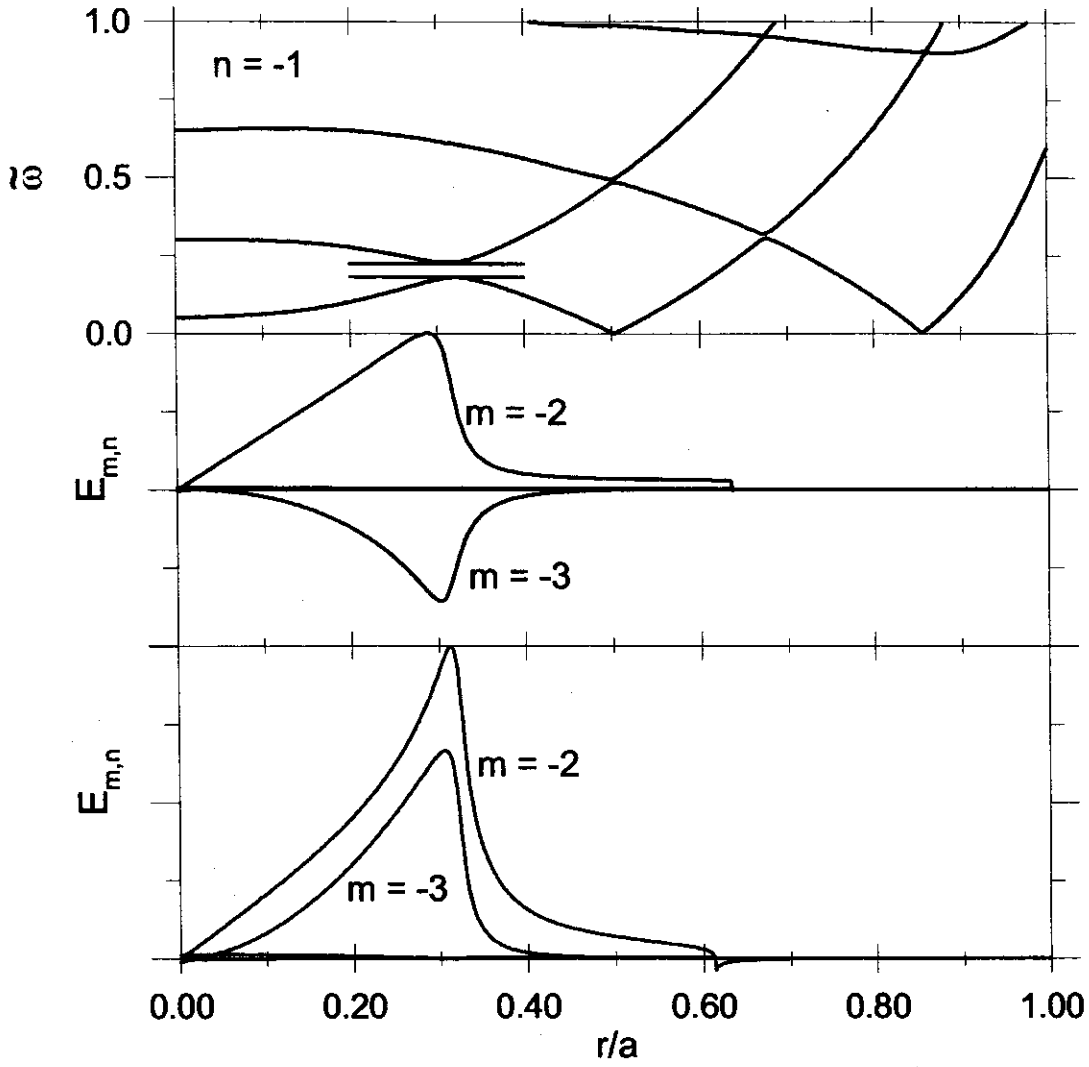

FIG. 8. The calculated even and odd TAE modes in the LHD shot #24512. The ratio of eigenfrequencies is 1.236, which agrees with experimental data.

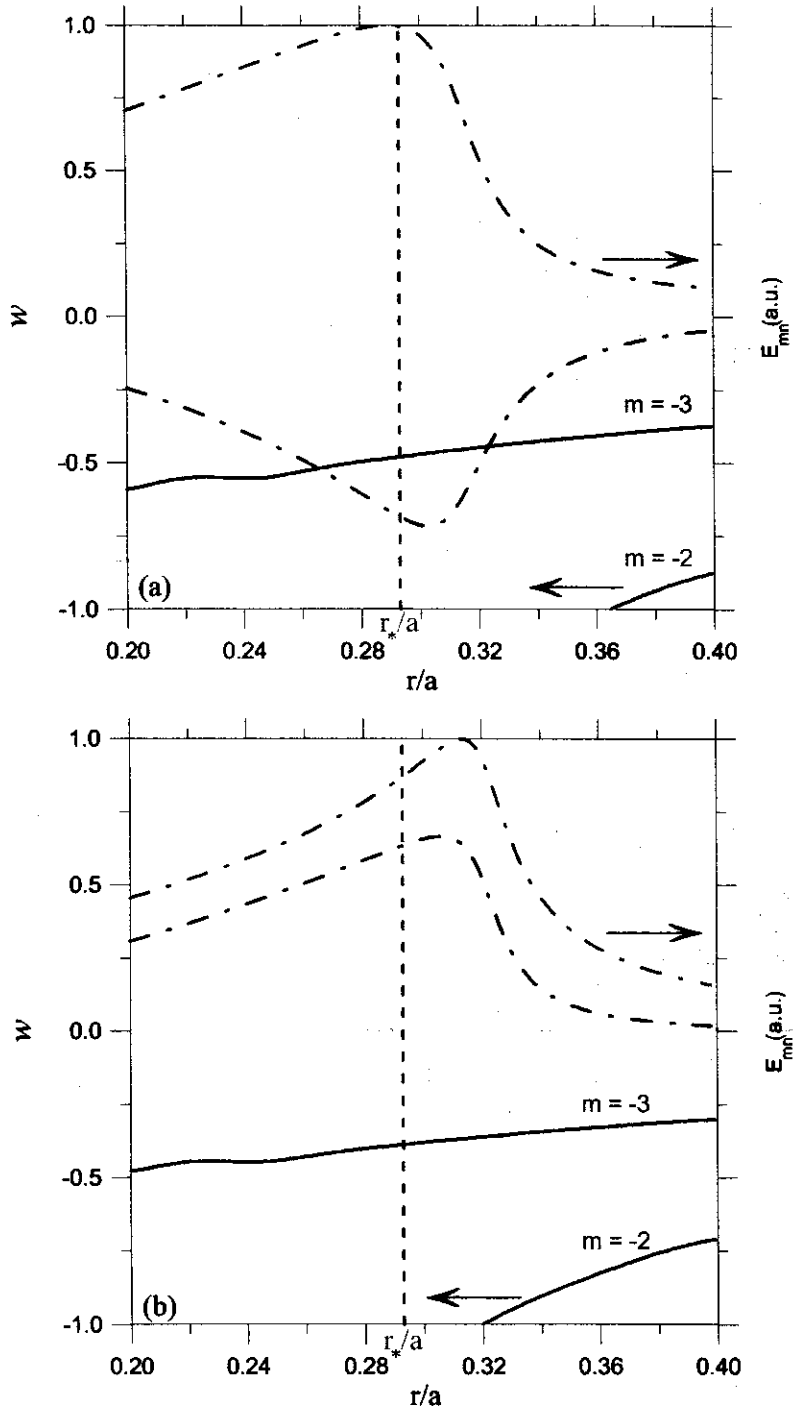

FIG. 9. The normalized resonant velocities (w) shown by solid lines for the dominant components of the even and odd TAE modes in the LHD shot #24512: (a), the odd mode; (b), the even mode. Dashed-dotted lines show the mode amplitudes. We observe that there are no resonant particles at $r = r_*$, whereas in the lower figure the resonant particles with $|w| \sim 1$ appear at $r/a \approx 0.32$, where the radial derivative of the mode amplitude is large.

Recent Issues of NIFS Series

NIFS-760 T. Hayashi, N. Mizuguchi, H. Miura, R. Kanno, N. Nakajima and M. Okamoto
Nonlinear MHD Simulations of Spherical Tokamak and Helical Plasmas
Oct. 2002 (TH/6-3)

NIFS-761 K. Yamazaki, S. Imagawa, T. Muroga, A. Sagara, S. Okamura
System Assessment of Helical Reactors in Comparison with Tokamaks
Oct. 2002 (FT/P1-20)

NIFS-762 S. Okamura, K. Matsuoka, S. Nishimura, M. Isobe, C. Suzuki, A. Shimizu, K. Ida, A. Fujisawa, S. Murakami, M. Yokoyama, K. Itoh, T. Hayashi, N. Nakajima, H. Sugama, M. Wakatani, Y. Nakamura, W. Anthony Cooper
Physics Design of Quasi-Axisymmetric Stellarator CHS-qa
Oct. 2002 (IC/P-07)

NIFS-763 Lj. Nikolic, M.M. Skoric, S. Ishiguro and T. Sato
On Stimulated Scattering of Laser Light in Inertial Fusion Energy Targets
Nov. 2002

NIFS-764
NIFS Contributions to 19th IAEA Fusion Energy Conference (Lyon, France, 14-19 October 2002)
Nov. 2002

NIFS-765 S. Goto and S. Kida
Enhanced Stretching of Material Lines by Antiparallel Vortex Pairs in Turbulence
Dec. 2002

NIFS-766 M. Okamoto, A.A. Maluckov, S. Satake, N. Nakajima and H. Sugama
Transport and Radial Electric Field in Torus Plasmas
Dec. 2002

NIFS-767 R. Kanno, N. Nakajima, M. Okamoto and T. Hayashi
Computational Study of Three Dimensional MHD Equilibrium with m/n=1/1 Island
Dec. 2002

NIFS-768 M. Yagi, S.-I. Itoh, M. Kawasaki, K. Itoh and A. Fukuyama
Multiple-Scale Turbulence and Bifurcaion
Jan. 2003

NIFS-769 S.-I. Itoh, K. Itoh and S. Toda
Statistical Theory of L-H Transition and its Implication to Threshold Database
Jan. 2003

NIFS-770 K. Itoh
Summary: Theory of Magnetic Confinement
Jan. 2003

NIFS-771 S.-I. Itoh, K. Itoh and S. Toda
Statistical Theory of L-H Transition in Tokamaks
Jan. 2003

NIFS-772 M. Stepic, L. Hadzievski and M.M. Skoric
Modulation Instability in Two-dimensional Nonlinear Schrodinger Lattice Models with Dispersion and Long-range Interactions
Jan. 2003

NIFS-773 M.Yu. Isaev, K.Y. Watanabe, M. Yokoyama and K. Yamazaki
The Effect of Hexapole and Vertical Fields on α-particle Confinement in Heliotron Configurations
Mar. 2003

NIFS-774 K. Itoh, S.-I. Itoh, F. Spineanu, M.O. Vlad and M. Kawasaki
On Transition in Plasma Turbulence with Multiple Scale Lengths
May 2003

NIFS-775 M. Vlad, F. Spineanu, K. Itoh, S.-I. Itoh
Intermittent and Global Transitions in Plasma Turbulence
July 2003

NIFS-776 Y. Kondoh, M. Kondo, K. Shimoda, T. Takahashi and K. Osuga
Innovative Direct Energy Conversion Systems from Fusion Output Thermal Power to the Electrical One with the Use of Electronic Adiabatic Processes of Electron Fluid in Solid Conductors.
July 2003

NIFS-777 S.-I. Itoh, K. Itoh and M. Yagi
A Novel Turbulence Trigger for Neoclassical Tearing Modes in Tokamaks
July 2003

NIFS-778 T. Utsumi, J. Koga, T. Yabe, Y. Ogata, E. Matsunaga, T. Aoki and M. Sekine
Basis Set Approach in the Constrained Interpolation Profile Method
July 2003

NIFS-779 Oleg I. Tolstikhin and C. Namba
CTBC A Program to Solve the Collinear Three-Body Coulomb Problem: Bound States and Scattering Below the Three-Body Disintegration Threshold
Aug. 2003

NIFS-780
Contributions to 30th European Physical Society Conference
on Controlled Fusion and Plasma Physics
(St.Petersburg, Russia, 7-11 July 2003)
from NIFS
Aug. 2003

NIFS-781 Ya. I. Kolesnichenko, K. Yamazaki, S. Yamamoto, V.V. Lutsenko, N. Nakajima, Y. Narushima, K. Toi, Yu. V. Yakovenko
Interplay of Energetic Ions and Alfvén Modes in Helical Plasmas
Aug. 2003

Printed on 100% Recycled Paper for this Text